Titre: Title:	Monitoring System for the Online Estimation of the Internal Parameters of a Microbial Fuel Cell Operated Intermittently
Auteur: Author:	Javier Dario Coronado
Date:	2013
Type:	Mémoire ou thèse / Dissertation or Thesis
Référence: Citation:	Coronado, J. D. (2013). Monitoring System for the Online Estimation of the Internal Parameters of a Microbial Fuel Cell Operated Intermittently [Mémoire de maîtrise, École Polytechnique de Montréal]. PolyPublie. https://publications.polymtl.ca/1296/

URL de PolyPublie: PolyPublie URL:	https://publications.polymtl.ca/1296/
Directeurs de recherche: Advisors:	Michel Perrier, & Boris Tartakovsky
Programme: Program:	Génie chimique

UNIVERSITÉ DE MONTRÉAL

MONITORING SYSTEM FOR THE ONLINE ESTIMATION OF THE INTERNAL PARAMETERS OF A MICROBIAL FUEL CELL OPERATED INTERMITTENTLY

JAVIER DARIO CORONADO

DÉPARTEMENT DE GÉNIE CHIMIQUE

ÉCOLE POLYTECHNIQUE DE MONTRÉAL

MÉMOIRE PRÉSENTÉ EN VUE DE L'OBTENTION

DU DIPLÔME DE MAÎTRISE ÈS SCIENCES APPLIQUÉES

(GÉNIE CHIMIQUE)

NOVEMBRE 2013

UNIVERSITÉ DE MONTRÉAL

ÉCOLE POLYTECHNIQUE DE MONTRÉAL

Ce mémoire intitulé :

MONITORING SYSTEM FOR THE ONLINE ESTIMATION OF THE INTERNAL PARAMETERS OF A MICROBIAL FUEL CELL OPERATED INTERMITTENTLY

présenté par : CORONADO Javier Dario

en vue de l'obtention du diplôme de : Maîtrise ès Sciences Appliquées

a été dûment accepté par le jury d'examen constitué de :

M.SRINIVASAN Bala, Ph. D., président

M. PERRIER Michel, Ph. D., membre et directeur de recherche

M. TARTAKOVSKY Boris, Ph. D., membre et codirecteur de recherche

Mme. WOODWARD Lyne, Ph. D., membre

ACKNOWLEDGEMENT

Well, when it comes down to saying thanks, I just open my heart to all those I am grateful to. I have always thought that gratefulness only achieves its real value when it is communicated from the heart. I will only translate my acknowledgement words for you, Michel and Boris. Please try the Spanish version, it is much more beautiful.

Some years ago, I had the chance to read a book in Strategy consulting that finished by giving an advice: "Wherever you go in life, always find a mentor". Recently, life gave me the chance to add 2 very special people to a very long list of very beloved mentors: Michel, and Boris. Michel: without realizing it, you brought fun to my life in a moment in which it was actually difficult to find. I will always be grateful to you for having trusted me when I most needed it. Simply, THANK YOU SO MUCH! Boris: if it was not for your advice, and respect (patience!) for my ideas (passionate, though not always structured), besides all the trust you always had in my work, half of the results in this document would have never been possible. I will always be grateful for your unconditional support.

A la hora de los agradecimientos, no suelo guardarme nada. Quizás algunos lo sepan, otros quizás no, pero soy un convencido de que la gratitud sólo alcanza su verdadera grandeza cuando se expresa de corazón. Por ello, estas palabras son para ustedes:

Hace unos años, tuve la oportunidad de leer un libro de estrategia que en su último capítulo aconsejaba: “a donde vayas, busca siempre un mentor”. Más tarde en la vida caí en cuenta que siempre he gozado de excelentes mentores. Al nacer, la vida me bendijo con los que han sido mis 2 mayores pilares: papá y mamá. A ustedes les debo todo cuanto soy. Este paso en mi vida se los comparto, como les he compartido muchos otros. Sin duda, de no ser por todo lo que ustedes me inculcaron, hoy por hoy yo no sería quien soy.

Más recientemente, la vida trajo a mí dos personas que desde ya hacen parte de esa lista de espectaculares mentores: Michel y Boris. Michel: sin saberlo, trajiste diversión a mi vida en un momento en el que me era difícil encontrarla. Siempre te estaré agradecido por haberme dado un voto de confianza cuando más lo necesitaba. Sencillamente, ¡MUCHAS GRACIAS! Boris: de no ser por tus consejos, tu respeto (¡y paciencia!) por mis ideas (apasionadas, más no siempre estructuradas), además de toda la confianza que depositaste en mi trabajo, la mitad de los

resultados en este documento no hubieran sido posibles. Siempre te estaré agradecido por todo tu apoyo incondicional.

A toda la colonia colombiana en Polytechnique (¡todos!), muchas gracias por muy agradables momentos juntos. Quebeca: si no me hubiera contigo en aquel ya lejano 2010, no hubiese caido en cuenta de que aún tenía por descubrir una de mis grandes pasiones en la vida: la ingenieria química. ¡Gracias!

Un párrafo aparte para quien ha sido mi compañero de batalla en todas éstas: ¡Chucho! Mi hermano, si no hubiera chupado de su sangre todos estos años, nada de esto sería posible. Gracias por toda su paciencia y tolerancia. Yo sé que no es fácil lidiar conmigo. Usted lo sabe… Estoy trabajando en un milagro del que usted hace parte integrante. Si mi intuición no me engaña, la vida nos depara aún muchas otras batallas de las cuales sé que habremos de salir vencedores.

Por último, más no por ello menos importante: ¡Tú! Sí… ¡Tú! ¡Ángela! Este triunfo es tan tuyo como mío… Tú eres la responsable de todos y cada uno de los anteriores párrafos. Nunca antes dediqué un documento a nadie. Bueno, ¡pues éste es para ti! No me alcanzan las palabras para darte las gracias…

¡MUCHAS GRACIAS A TODOS!

RÉSUMÉ

Cette étude décrit l'opération des Piles à Combustible Microbiennes (PCMs) avec la connexion intermittente de la résistance externe (mode R-PWM). L'étude est composée de 2 sections : la première décrit l'opération de la PCM à basses et hautes fréquences, avec différents taux de connexion/déconnexion de la résistance externe. La deuxième partie rejoint le mode de fonctionnement RPWM à la solution analytique d'un Modèle de Circuit Équivalent (MCE), afin de développer une procédure de supervision en ligne. Cette stratégie rend le suivi périodique des paramètres internes de la PCM possible.

Quant à la première partie du projet, l'analyse des profils de tension acquis démontrent la présence de composants dynamiques lents et rapides. Ceux-ci peuvent être décrits par un modèle de circuit équivalent simple, qui est d'ailleurs approprié pour des applications comme la commande de procédés. Aux fréquences d'exploitation plus élevées que 100 Hz, une amélioration considérable de la performance des PCMs est observée, avec une augmentation du 22 % au 43 % de la puissance de sortie, en comparaison avec l'opération de la PCM avec sa résistance externe continuellement connectée.

Basé sur les dynamique identifiées pour la PCM à basse et haute fréquence, la solution analytique pour le modèle de circuit équivalent est ensuite utilisée comme base pour développer une stratégie de supervision en ligne. L'algorithme permet le calcul en ligne des paramètres internes de la PCM. Pour valider l'exactitude des valeurs estimées, les profils de tension électrique à bas et haute fréquence sont générés et statistiquement comparés aux profils réels de tension de la PCM. Quand les 2 profils sont comparés, des erreurs quadratiques moyenne de $5.26e^{-4}$ sont obtenues pour les profils de basse fréquence. À haute fréquence, l'erreur est $9.69e^{-6}$. Par ailleurs, les estimations en ligne des paramètres internes sont comparées à des paramètres calculés hors ligne. Les évolutions observées sont en effet semblables, même si les valeurs diffèrent.

La stratégie de supervision en ligne a été testée sous 2 conditions d'opération différentes : d'abord, une PCM a été utilisé dans pour étudier l'évolution des paramètres en réponse aux changements de la charge organique. De plus, une deuxième PCM a été construite pour faire le suivi périodique de l'évolution des paramètres internes dans le temps, du démarrage de la PCM à sa maturité.

ABSTRACT

This research study describes the operation of a Microbial Fuel Cell (MFC) under pulse-width modulated connection of the external resistor (RPWM mode). The study is composed of 2 main sections: the first one describes the MFC operation at low and high frequencies, and under varying periods of external resistance connection/disconnection or duty cycle (*D*). The second part blends the RPWM mode of operation to the analytical solution of a proposed Equivalent Circuit Model (ECM) in order to develop an on-line monitoring procedure. This monitoring strategy allows the periodic follow-up of the MFC internal parameters.

Regarding the first part of this project, the analysis of the output voltage profiles acquired during R-PWM tests showed the presence of slow and fast dynamic components, which can be described by a simple equivalent circuit model (ECM) suitable for process control applications. At operating frequencies above 100 Hz a noticeable improvement in MFC performance was observed with the power output increase of 22–43% as compared to MFC operation with a constant external resistance.

Based on the identified dynamics for the MFC dynamics at low and high frequency, the analytical solution for the equivalent circuit model is used as a basis for an on-line monitoring strategy. This algorithm allows the online estimation of the MFC internal parameters. To validate the accuracy of the estimations, low and high frequency voltage profiles are generated and statistically compared to actual voltage profiles for the MFC. When actual and online estimated profiles are compared, mean square errors of 5.26e-4 for low frequency profiles, and 9.69e-6 for high frequency profiles were obtained. On-line estimations of the MFC internal parameters are also compared to off-line estimated parameters, and similar evolution trends are observed.

The on-line monitoring strategy was tested under 2 different operating conditions: first, one MFC was used in under to study parameter evolution under varying organic load. Then, a second MFC was newly built in order to make a periodic follow-up of the internal parameters' evolution in time, from the MFC start-up to its maturity.

CONDENSÉ

Introduction et objectives

Les Piles à Combustible Microbiennes (PCMs) sont considérées une solution technologique prometteuse dans la recherche de nouvelles sources d'énergie renouvelables, capables de remplacer des combustibles fossiles comme source d'énergie principale des humains. En général, une pile à combustible est définie comme un dispositif électrochimique avec la capacité de convertir l'énergie chimique directement en électricité. Quoique des réactions chimiques ayant lieu dans des piles à combustible soient semblables à ceux ayant lieu dans des batteries conventionnelles, la différence principale entre ces deux vient du fait que les piles à combustible sont des systèmes ouverts où les réactifs coulent continuellement dans la pile.

Même si les PCMs ne pourront pas remplacer le pétrole dans un futur proche, leur capacité à produire de l'énergie électrique les rend un sujet de recherche intéressant. Étant un système bio-électrochimique, les PCMs ont déjà prouvé leur capacité à produire de l'électricité, ainsi qu'à traiter des eaux usées (Oh, et d'autres., 2010). C'est pourquoi, des sciences multiples se mêlent présentement dans leur étude : la microbiologie, la chimie, le génie chimique, le génie électrique, le génie civil, ainsi que les sciences des matériaux sont en fait le cas. Néanmoins, un des plus grands défis scientifiques est toujours lié à la modélisation et au contrôle, étant donné la nature toujours changeante des systèmes vivants.

Ce document présente alors les résultats obtenus du projet de recherche visant à développer un outil de supervision en temps réel pour l'analyse en ligne de la performance électrique d'une Pile à Combustible Microbienne opérée de façon intermittente. Afin d'atteindre cet objectif, deux tâches principales sont exécutées:

1. la caractérisation de la performance électrique de PCMs opérées de façon intermittente en fonction de la fréquence d'opération et du ratio de connexion/déconnexion de la résistance externe, et
2. le développement d'un outil de supervision en ligne pour évaluer les paramètres internes électriques d'une PCM modélisée à partir d'un modèle de circuit équivalent (MCE) simplifié.

Mode R-PWM et caractérisation en fréquence

Afin d'évaluer l'effet de la connexion intermittente de la résistance externe (mode d'opération R-PWM), deux (2) PCMs ont été opérées à plusieurs fréquences dans une plage entre 0.1 Hz et 1000 Hz. À chaque fréquence testée, R_{ext} est connectée à la PCM pendant la première moitié du cycle et débranché pour le reste du cycle. Ces tests ont été effectués pour des valeurs de R_{ext} entre 8 et 47 ohms. La tension moyenne a augmenté avec l'augmentation de fréquence, ensuite un plateau est atteint à peu près entre 100 et 500 Hz.

Aux fréquences d'exploitation plus élevées que 100 Hz, une amélioration considérable de la performance des PCMs est observée, avec une augmentation du 22 % au 43 % de la puissance de sortie, en comparaison avec l'opération de la PCM avec sa résistance externe continuellement connectée.

MCE et les dynamiques à basse et haute fréquence

À basse fréquence (~0.05 Hz) deux composants dynamiques différents sont remarqués lors de la connexion intermittente de la résistance externe. D'abord, il y a un changement soudain de la tension de sortie de la PCM, jusqu'à atteindre d'une certaine valeur intermédiaire. Cette transition rapide est suivie par une courbe exponentielle, qui s'approche de la valeur stationnaire à un taux beaucoup plus lent.

Par contre à haute fréquence (~100 Hz), seulement la dynamique rapide apparaît dans le profil de tension de la PCM, alors que la dynamique lente disparaît et le voltage semble essentiellement commuter entre deux niveaux. La tension la plus haute correspond à l'état de circuit ouvert (résistance externe déconnectée). D'autre côté, la tension la plus basse correspond à l'état de circuit fermé (résistance externe connectée). Ces deux (2) dynamiques peuvent être décrites par un modèle de circuit équivalent (Randles le modèle, (Randles, 1947)). Ce modèle consiste de deux résistances et une capacitance, qui permet la description des réponses de tension de sortie lentes et rapides observées pendant les tests. Pour le modèle montré dans la **¡Error! No se encuentra el origen de la referencia.** de ce document, U_{OC} correspond à la tension de circuit ouverte de la PCM (tension idéale), C représente la capacitance réelle de la MFC, R_1 représente les pertes ohmiques, alors que R_2 représente les pertes par activation et par concentration de la PCM (Yang, Zhang, Shimotori, Wang et Huang, 2012).

Le MCE et la stratégie de supervision en ligne

Généralement, les propriétés électriques de systèmes bio-électrochimiques sont mesurées au moyen des méthodes électrochimiques hors connexion comme des courbes de polarisation ou avec des voltamètres cycliques. Bien que ces méthodes fournissent des mesures précises pour des paramètres électriques comme la résistance interne et la capacitance, ils exigent que le système soit pris hors ligne pour la mesure pour être précis.

Dans le but de pouvoir appliquer les principes de commande de procédé à l'amélioration de la performance des PCMs, il est nécessaire d'avoir des outils permettant le suivi en ligne des paramètres internes des PCMs. La stratégie de supervision proposée dans ce projet de recherche est basée tant sur la solution analytique du modèle de circuit équivalent étudié (MCE), que sur les profils à bas et haute fréquence retrouvés lors de l'opération intermittente de la PCM.

La stratégie de supervision en ligne a été testée pour deux (2) conditions d'opération différentes : d'abord, l'évolution des paramètres en réponse aux changements de la charge organique a été étudié. Ensuite, l'évolution des paramètres internes dans le temps est étudiée, en suivant le comportement dynamique d'une PCM du démarrage à sa maturité.

L'algorithme permet en effet le calcul en ligne des paramètres internes de la PCM. Pour valider l'exactitude des valeurs estimées, les profils de tension électrique à bas et haute fréquence sont générés et statistiquement comparés aux profils réels de tension de la PCM. Quand les 2 profils sont comparés, des erreurs quadratiques moyenne de 5.26e-4 sont obtenues pour les profils de basse fréquence. À haute fréquence, l'erreur est 9.69e-6. Par ailleurs, les estimations en ligne des paramètres internes sont comparées à des paramètres calculés hors ligne.

TABLE OF CONTENTS

LIST OF TABLES

LIST OF FIGURES

LIST OF ABBREVIATIONS

D	Duty Cycle
DC	Direct Current
ECM	Equivalent Circuit Model
MCE	Model de Circuit Équivalent
MSE	Mean Square Error
MFC	Microbial Fuel Cell
MPPT	Multi-unit Maximum Power Point Tracking
PCM	Pile à Combustible Microbienne
P/O	Perturbation / Observation Algorithm
PWM	Pulse Width Modulation
R-PWM	Resistance-Pulse Width Modulation mode

CHAPTER 1 INTRODUCTION

Just like every living form on Earth, human beings are constantly changing. That is why, evolving has always been deep in our nature. Nevertheless, growth transitions, like adolescence, often cause problems to humans. Adaptive behavior is needed in order to catch up with new circumstances. Moments of transition always represent great challenges for human's creativity and adaptability. Nowadays, humanity is hugely concerned by a great moment of transition that challenges our scientific and technological knowledge. Maybe for the very first time in our young history, the challenge embraces human's capacity to sustainably live in a society.

Human's need for sustainable development imperatively demands: 1) the change of our highly non-renewable and contaminating energy sources by renewable ones; 2) the optimization of wastewater treatment procedures, as well as 3) the efficiency improvement of the energy recovery techniques currently in use in industry. Beautifully, the challenge has not only attracted the attention of scientists around the world, but it has been the main reason for multiple television series and science fiction films for the last two decades. AVATAR, IRON MAN, BATMAN or PRISON BREAK are just a small proof of it.

Microbial Fuel Cells (MFCs) are considered a promising technological solution that could help tackling the challenges previously mentioned. Even though MFCs are not yet considered an energy source capable of replacing petroleum based fuels in a foreseeable future, their capacity for electrical energy recovery make them an interesting subject for research. As a bio-electrochemical system, MFCs have already proven their capacity to generate electricity while biochemically treating wastewater (Oh, et al., 2010). Hence, multiple sciences have merged in their study: microbiology, chemistry, chemical, civil, and electrical engineering, as well as material science. Nonetheless, one of the biggest scientific challenges is always tied to the modeling and control of the continually changing nature of the oxidation-reduction reactions taking place in the bioreactors.

For the case of study described in this document, chemical and electrical engineering gather together once again in the quest for a beautiful goal: modeling, optimizing and controlling MFCs. This fusion have proven extraordinary results for science in the past, giving even birth to heat transfer modeling by means of basic first order electrical circuits (Bergman, Lavine, Incropera, & Dewitt, 2012). So, just as heat exchangers were initially studied using electrical

models to later become a major energy recovery tool in industrial process plants, electrical circuits are currently used as a modeling tool in the research to attain a major understanding of inherently living systems such as the MFCs.

Therefore, the research presented in this document looks forward to improving human's understanding of MFCs by using some engineering tools to study them, while improving their performance. For sure, MFCs are foreseen as a feasible technology for electrical energy recovery in the search for reducing electrical energy consumption in wastewater treatment plants. Power efficiency improvement has become a common issue in current research studies.

Hereafter, some major concepts are presented. These represent the major scientific framework inside which this research has been developed. Besides, they create a technical framework prior to introducing the main objectives of this research project.

1.1 Problem Definition

1.1.1 Microbial Fuel Cells

In general, a fuel cell is defined as an electrochemical device with the capacity to directly convert chemical energy into electricity. Though chemical reactions taking place in fuel cells are similar to those occurring in conventional batteries, the main difference between these two arises from the fact that fuel cells are open systems where reactants are continually flowing into the cell.

Oxidation-Reduction reactions take place in fuel cells. Oxidation takes place at the anode, known by convention as the negative electrode, while reduction takes place at the cathode, the positive electrode. When reaction takes place, electrons are liberated, allowing current to flow between both electrodes. To foster ion exchange, the electrodes are commonly placed in an electrolyte solution.

In the particular case of MFCs, electricigenic microorganisms work as the catalysers of the bio-electrochemical reaction. Wastewater containing dissolved organic matter may be used as fuel for the cell. The organic matter is degraded by these microorganisms, which need this material for their biological cycle that comprises their metabolism, growth and reproduction.

1.1.2 Microbial Fuel Cells and Water Treatment

MFCs are a new type of bioreactors with a proven capacity for treating a large variety of highly diluted organic matter while producing electricity (Logan & Regan, 2006); (Debabov, 2008).

In general, MFCs are composed of two chambers: the anaerobic anode, and the aerobic cathode. These two are separated by an ion conducting membrane. Anaerobic respiring bacteria attached to the anode work as catalysers, while oxidizing organic matter and producing both protons and electrons. The electrons are transferred to the anode, where they subsequently pass through an external electrical circuit to produce current. Protons migrate through the membrane to the cathode, where they react with oxygen to produce water.

Research on MFCs may be divided into three main areas (Oh, et al., 2010):

1) the reactor design in order to reduce unwanted biomass production in wastewater treatment,
2) the study of the microbial communities participating in the bio-electrochemical process, and
3) modeling, control and optimization of operating conditions.

One of the main goals of applying control and optimization techniques is the enhancement of MFCs low power density (Logan, et al., 2006).

1.1.3 Dynamic Systems, Process Control and Frequency Analysis

Systems in engineering are studied in two different ways: dynamically and statically. Dynamic models comprise both transient and steady state responses, while static systems are commonly studied in order to identify the steady state response of a given system. Dynamic models are commonly represented by differential equations in a time based space, while different frequency space transformations (Fourier, Laplace, etc.) are highly used in order to make stability analysis in a frequency based space.

Commonly, when a dynamic model is achievable, control laws are established in order to improve the performance of the system. In the case of biochemical systems, as it is the case for MFCs, models are difficult to develop due to their highly non-linear time variant inherent characteristic.

In the case of MFCs, electrical studies have been carried out neglecting fast dynamics related to electrical properties of the MFCs (Aelterman, Versichele, Marzorati, Boon, & & Verstraete, 2008); (Woodward, Perrier, Srinivasan, & Tartakovsky, 2009)). These research studies model MFCs as electrical systems by means of exclusively resistive circuits. More recently, MFCs electrical dynamics has been paired to first order circuits (Yang, Zhang, Shimotori, Wang, & Huang, 2012). Furthermore, periodic operation of MFCs is currently being studied in order to improve MFCs power generation capacity, as well as for modelling their transient response (Grondin, Perrier, & Tartakovsky, 2012); (Coronado, Perrier, & Tartakovsky, 2013).

When dynamic systems are modeled, low and high frequency analysis become very useful as a stability analysis and modeling tool. Besides, frequency based methods make it possible to accurately establish the frequency response of electrically modeled systems. Different frequency-based methods used in process control comprise: bode diagrams, root-locus representation, and Nyquist stability analysis, among others.

1.1.4 Pulse Width Modulation (PWM) and Power Control

Pulse Width Modulation (PWM) is a control technique commonly used for power control in power electronic applications. In these applications, the average power to a load is controlled by commuting on and off an electronic power switching device. As voltage (and current) coming out of the power source are modulated (switched 'on' and 'off'), power is controlled so maximum power feed may be achieved, subsequently optimizing the energy furnished to the attached load.

Duty cycle (D) corresponds to the portion of 'on' time to the period of time. It is commonly expressed in percent. Generally, low power corresponds to a low duty cycle, while 100% means that the circuit is always 'on'. PWM is a well-known electrical control technique already under study on MFCs, mainly looking forward to enhancing the system's energy storage capacity (Wu, Biffinger, Fitzgerald, & Ringeisen, 2011).

1.2 Project Objectives

General Objective: To develop a real-time process monitoring tool for the on-line analysis of the electrical power performance of a Microbial Fuel Cell operated intermittently.

Specific Objectives:

1) Characterize the performance of a MFC operated intermittently as a function of the external resistance connection/disconnection rate (variable frequency and duty cycle).
2) Develop an on-line monitoring tool for estimating electrical internal parameters of a MFC modeled using a simplified equivalent circuit model (ECM).

1.3 Document Structure

After presentation the literature review and the material and methods that give a frame to this project, the main research results are presented in chapters 4 and 5.

Chapter 4 mainly explains the proposed method of operation for the MFC (R-PWM). Two main studies are presented: the characterisation of MFC power performance to an intermittent operation at low and high frequencies, as well as the MFC power performance in response to varying period of connection or duty cycle (D). Besides, the Equivalent Circuit Model (ECM) is first explained, creating the links between this model and the MFC operation at low and high frequencies.

Chapter 5 describes the way in which the analytical solution of the ECM is used in order to achieve an on-line monitoring and parameter estimation algorithm. The results for 2 different experiences are presented. First, the on-line monitoring strategy is used to make the follow-up of MFC internal parameters while organic load is periodically varied. Second, a MFC was newly built and followed-up by means of the propose on-line parameter estimation procedure. The evolution of parameters in time is then evaluated.

Finally, the conclusions to the study presented in this document are mainly focused on the results presented in Chapters 4, and 5.

CHAPTER 2 LITERATURE REVIEW

This literature review is composed of three main sections. The first one makes a brief overview of the principles of biochemical processes. Then, the second section describes how modeling of MFCs has evolved in time, while the last section summarizes some state-of-the-art studies on MFCs optimization and control.

1.4 Biochemical Processes: an overview

Basically, a biochemical process is focused on the growth of certain type of microorganism. In order for a microorganism to grow, nutrients must be fed at favourable environmental conditions (temperature, pH, etc.). Hence, while the biochemical process takes place, a carbon source (substrate) is consumed in order to produce such products as oils, cheeses, enzymes, amino acids, ethanol or biogas, among others, depending on the main interest of the corresponding industry.

Modeling a biochemical system is a critical stage prior to its optimization and control. A biochemical reaction scheme is initially established in order to describe the biological and chemical reactions that take place in the bioreactor. Reactions belonging to the reaction scheme may include: microorganisms' growth, product generation, and microorganisms' mortality. Schemes are normally completed (Bastin, et al., 2001) by including the reactions' rates and the consumption yields. Reaction kinetics are often modelled by means of a Monod model, which is based on the Michaelis-Menten reaction kinetics (Eddy, 2003).

Reaction's schemes are completed with mass and energy balances. In fact, these schemes make it possible to establish dynamical models for the biochemical system. Mass balances are highly dependent on the type of reactor used (batch, fed batch or continuous stirring tank reactor (CSTR)). Balances are normally expressed as a function of different variables (substrates, products or biomasses) that describe the dynamics of the system. Finally, reaction rates are expressed as a function of the chosen variables for simulation, control or optimization purposes.

1.5 Microbial Fuel Cells Modeling: from Microbiology to Process Dynamics

Microbial fuel cells (MFCs) are based on biochemical processes in which electricity is a final product for the reacting system (scheme). The main challenge arising while modeling MFCs is the adequate interpretation of the narrow relationship between microbial growth and metabolism, and electricity generation and performance.

Although MFCs were initially modeled as one-population microbial systems, (Zhang & Halme, 1995); (Marcus, Torres, & Rittmann, 2007)), more recent studies (Picioreanu, Katuri, Head, Van Loosdrecht, & Scott, 2008) proved the need for multi-population biological models in order to accurately understand the biological behaviour inside the bioreactors used for MFCs' applications. Nonetheless, the complexity associated with multi-population models makes necessary to design simplified models for control and optimization purposes.

A simplified two-population bio-electrochemical model was proposed by Pinto et al., (Pinto R. P., Srinivasan, Manuel,, & Tartakovsky, 2010.) for off-line process optimization. The proposed model describes the competition of two types of microbial populations for a common substrate in a MFC: anodophilic and methanogenic bacteria. By means of multiplicative (double-Monod) models (Bae & Rittmann, 1996a), and Nernst based equations ("Fuel Cell Handbook," 2005), the model proposes a dependence of electrical parameters on anodophilic biomass density, besides proving the influence of organic load and external resistance on power output and long-term performance.

1.6 Microbial Fuel Cells: Performance Optimization, Energy Storage, and Control

Given their low power density (Logan, et al., 2006), researchers currently dedicate their research work to the development of optimization strategies allowing to increase their capacity for electrical energy production

.

1.6.1 Performance optimization

Different approaches are used in order to improve MFCs' performance. Some of them are related to Material Science and focus on improving bioreactor's performance. Some others seek a deeper understanding of the bio-electrochemical behaviour of the dynamic system.

A recent study aimed at improving bioreactor's performance demonstrates that using extended longitudinal tubular MFCs reactors may increase power recovery and organic removal efficiency (Kim, et al., 2011). Moreover, in (Saito, et al., 2011), the effect of carbon clothes anodes modified with 4(N,N-dimethylamino)benzene diazonium tetrafluoroborate over MFCs' performance is proved by demonstrating that the lowest the amount of nitrogen source in the anode, the highest maximum power density may then be achieved.

Aelterman et al., (Aelterman, Rabaey, Pham, Boon, & Verstraete, 2006) developed some tests with stacked microbial fuel cells in order to improve continuous electricity generation at high voltages and currents. The study proves the capacity of their approach to increase the values of both voltage and current, noting that microbial communities concentration are affected by the biological and electrochemical interactions between MFCs.

Moreover, substrate consumption has been optimized by means of staging strategies. A reactors-in-series approach (staging) (Pinto, Tartakovsky, Perrier, & Srinivasan, 2010) has already been proven to optimize substrate consumption in a MFC. The staging strategy was used to resemble CSTRs in series to Plug Flow Reactors (PFRs) dynamics. From the point of view of influent treatment performance, connection in series proved to have better treatment capacities than the connection in parallel.

1.6.2 Energy Harvesting and Storage

Electrical energy storage is also of great interest for researchers. In order for MFCs to be able to feed electrical energy to actual electrical loads, it is necessary to increase their capacity for electricity generation. To do so, (Dewan, Donovan, Heo, & Beyenal, 2010) have already developed a Microbial Fuel Cell tester with the capacity to calculate the power of the MFC as a function of the time needed to charge an external capacitance that harvests the power supplied by

the MFC. Power is optimized by varying the capacitor value and the charging and discharging potentials.

The principles of electrical power switching supplies are also currently under study looking forward to improving the energy storage capacity of stacked MFCs. Wu et al,. (Wu, Biffinger, Fitzgerald, & Ringeisen, 2011) designed a DC/DC booster circuit in order to increase a typical operational voltage to produce a maximum output power. Values for the DC/DC circuit are optimized using a proposed procedure while power consumed by the circuit was reduced to a minimum.

Similarly, Yang et al. (Yang, Zhang, Shimotori, Wang, & Huang, 2012) used a Power Management System (PMS) in order to improve a MFC's energy harvesting capacity. Super capacitors' impedance were optimized for maximum average harvested power, while a circuit composed of a transformer and a DC/DC boost converter is designed to increase both voltage and current supplied to an electrical non-resistive load. The transformer-based PMS network designed by Yang et al. works at a lower voltage that other MFC PMS designs.

The internal equivalent circuit model used by Yang et al. (Yang, Zhang, Shimotori, Wang, & Huang, 2012) is identical to that used by Grondin et al. (Grondin, Perrier, & Tartakovsky, 2012), though for different research purposes, following different approaches for the calculation of the MFC internal current.

1.6.3 Control and Optimization

Control theory is originally based on human's will to control and regulate systems just as the human body biologically regulates itself. However, two major restrictions arise on bioprocesses control and optimization (Bastin, et al., 2001):

1) the living nature of bioprocesses makes them difficult to model by means of already highly developed scientific methods, and

2) the unavailability of sensors for the continuous measurement of variables such as biomass, substrate, or product concentration.

Despite this, control and optimization techniques are broadly considered in the research for strategies that give scientists a further understanding of MFCs as a bio-electrochemical system. Both of them combined have extensively proven their capacity to identify system's parameters by using advanced well-known mathematical methods, what makes them highly attractive for the characterization and optimization of MFCs. Some state-of-the art studies are presented hereafter.

While varying electrical load (impedance) attached to an MFC, Premier et al., (Premier, Rae Kim, Michie, Dinsdale, & Guwy, 2011) proved that the automatic control of the load helps increasing both the MFCs' power and efficiency. When comparing the results of automatically changing the load to those obtained while letting the load fixed, an improvement of 19.73% in the MFC's electrical power performance is obtained. Both experiences were executed for MFCs operating at the same organic load.

Woodward et al., (Woodward, Perrier, Srinivasan, & Tartakovsky, Maximizing Power Production in a Stack of Microbial Fuel Cells Using Multiunit Optimization Method, 2009) developed a Multi-unit Maximum Power Point Tracking (MPPT) algorithm that calculates the gradient using outputs of two identical MFCs. The MFCs are operated at different resistive loads and the power difference between them indicates the direction the gradient should follow. Although the Achilles' heel of the proposed method arises at stating that both MFCs as identical, Woodward et al., (Woodward, Perrier, & Srinivasan, Comparison of Real-Time Methods for Maximizing Power Output in Microbial Fuel Cells, 2010) proved that this method converges faster than a perturbation-observation (P/O) algorithm, which varies the value of the controlled variable in order to establish the optimal operating point.

Furthermore, Degrenne et al., (Degrenne, Buret, Allard, Bevilacqua, & P., 2012) operated ten identical single-chamber 1.3L MFCs following a MPPT algorithm to control an electrical converter in order to improving global MFC performance. Their MPPT algorithm mainly consisted of the regulation of the MFC voltage to one-third of the open circuit value. The results obtained for power output following the proposed method were quite similar to those obtained when using a (P/O) algorithm.

Recently, external electrical circuits optimization is increasingly being used for MFC's research. Park et al. (Park & Ren, Hysteresis controller based maximum power point tracking

energy harvesting system for microbial fuel cells, 2012) developed a hysteresis controller based MFC energy harvesting system. For this case study, both an energy harvesting network and a voltage boost converter were conceived. The proposed MPPT algorithm uses potentiometers for the hysteresis controller. Their strategy eliminates the need for external resistances and enables simultaneous maximum power point tracking and maximum MFC energy harvest in real-time.

Electrical circuit modeling is another strategy increasingly being studied in order to complete the highly complex multi-population models of the MFCs. Besides estimating internal parameters of an internal equivalent circuit model proposed, Grondin et al. (Grondin, Perrier, & Tartakovsky, 2012) use the duty cycle principle in order to optimize power output to a fixed resistive load.

The proposed method makes a duty cycle control based on voltage measurements for minimum and maximum output voltages. It was proven that power output may be maximized both under limiting or non-limiting organic load conditions, without changing the value of the external resistance, just by intermittently connecting the electrical load based on established voltage thresholds. This system achieved maximum power output at different duty cycle values, while the value of the external resistive load was changed.

Another duty cycle analysis over a MFC was made by Wu et al. (Wu, Biffinger, Fitzgerald, & Ringeisen, 2011). In this case, a duty cycle and a frequency analysis were made over a DC/DC booster circuit connected to the studied MFC. The frequency analysis was made from 10 to 50 kHz in order to establish the frequency at which maximum output power is achieved from 3 stacked mini-MFCs connected in parallel. In the case of study of Grondin et al. (Grondin, Perrier, & Tartakovsky, 2012), no frequency analysis is described, though frequencies used are $\sim 0.1\ Hz$.

CHAPTER 3 MATERIALS AND METHODS

1.7 MFC design, inoculation, and operation

Two membrane-less air-cathode MFCs were constructed using nylon plates as described elsewhere (Grondin et al. 2012). The anodes were 5 mm thick carbon felts measuring 10 cm × 5 cm (SGL Canada, Kitchener, ON, Canada) and the cathodes were 10 cm x 5 cm manganese - based catalyzed carbon E4 air cathodes (Electric Fuel Ltd, Bet Shemesh, Israel). The electrodes were separated by a nylon cloth. Two MFCs, MFC-1 and MFC-2, were built. Both MFCs had an anodic compartment volume of 50 mL. MFC-1 contained two 10 cm x 5 cm carbon felt anodes with a total thickness of 10 mm and two cathodes (one on each side connected by a wire) with a total surface area of 100 cm^2. MFC-2 had one 10 cm x 5 cm carbon felt anode with a thickness of 5 mm and one 50 cm^2 cathode.

Each MFC was inoculated with 5 mL of anaerobic sludge with volatile suspended solids (VSS) content of approximately 40-50 g L^{-1} (Lassonde Inc, Rougemont, QC, Canada) and 20 mL of effluent from (Pinto R. , Srinivasan, Guiot, & Tartakovsky, 2011a)an operating MFC. The MFCs were maintained at 25ºC and were continuously fed with sodium acetate and trace metal solutions using a syringe pump and a peristaltic pump, respectively. The acetate stock solution was composed of (in g L^{-1}): sodium acetate (37.0), yeast extract (0.8), NH_4Cl (18.7), KCl (148.1), K_2HPO_4 (64.0), and KH_2PO_4 (40.7). The infusion rate of the acetate stock solution was varied in order to obtain the desired influent concentration. The trace metal solution was prepared by adding one mL of the trace elements stock solution to 1 L of deionised water. A detailed composition of the stock solution of the trace elements is given elsewhere (Pinto R. , Srinivasan, Guiot, & Tartakovsky, 2011a).

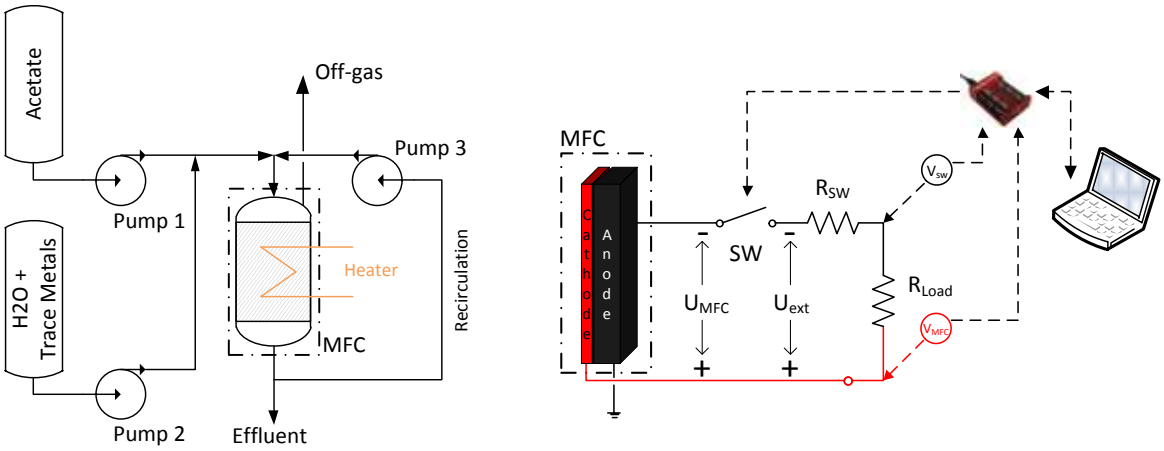

Figure 1. Schematic diagrams: (A) experimental setup, and (B) electrical circuit used in all tests.

An influent acetate concentration of 900 mg L^{-1} and a hydraulic retention time of 6-7 h were typically maintained, with an exception of the high and low-load tests, where the influent acetate concentration was varied. For organic load characterisation purposes, 4 different organic loads were used : 450 mg L^{-1}, 900 mg L^{-1}, 1350 mg L^{-1}, and 1800 mg L^{-1}. The mathematical calculation of acetate flow rates from these organic loads is later explained in this document. Figure 1A shows the schematic diagram of the experimental setup, while a detailed description of MFC design, stock solution composition, and operating conditions can be found elsewhere (Grondin, Perrier, & Tartakovsky, 2012).

1.8 External resistance connection (R-PWM Mode of Operation)

Pulse-width modulated connection of the external resistor (R_{ext}) to MFC terminals was achieved by adding an electronic switch (IRF540, International Rectifier, El Sequndo, CA, USA) to the external electrical circuit (denoted as SW in Figure 1B, the corresponding resistance is shown as R_{SW}). The switch was computer-controlled using a Labjack U3-LV data acquisition board (LabJack Corp., Lakewood, CO, USA). The data acquisition board was also used to record MFC voltage at a maximum rate of 22,500 scans/s.

As shown in Figure 1B, the data acquisition board measured MFC output voltage (U_{MFC}) and voltage after the switch (U_{sw}). Electrical connections corresponding to these measurements are shown in Figure 1B as V_{MFC} and V_{SW}, respectively. Voltage over the resistive load (U_{Load}) was calculated as the difference between U_{MFC} and U_{sw} ($U_{Load} = U_{MFC} - U_{sw}$). Electric current was calculated as $I = U_{Load} / R_{Load}$ by applying Ohm's law over the external load resistance (R_{Load}).

For calculation purposes, the switching device was considered as an ideal switch in series with a resistance R_{sw} to represent power losses in the switch. R_{sw} value was estimated by dividing the voltage over the switch by the current. In the following discussion, R_{ext} denotes the sum of the external load connected to the circuit and the switch resistance ($R_{ext} = R_{Load} + R_{sw}$) with a corresponding external voltage U_{ext}, as follows from the diagram shown in Figure 1B. The voltage measurements described above and the calculation method accounted for power losses due to the fast switching.

1.9 Frequency and Duty Cycle Tests

Frequency and duty cycle tests were carried out with either 15 min or 1 h intervals between parameter changes. The tests were performed in a broad range of frequencies from 0.1 Hz to 1000 Hz. Duty cycle was set to 50% when frequency tests were carried out. For the duty cycle analysis, duty cycles were varied between 5% and 100% at a constant frequency of 500 Hz. Between the R-PWM tests, the MFCs were operated using the Perturbation/Observation algorithm described below.

MFC performance was expressed in terms of average (per cycle) output voltage, current, and power output. Average values per cycle were obtained as follows:

$$M = \frac{1}{T}\int_0^T m(t)dt \qquad (1)$$

Where $m(t)$ is either the voltage, current, or power measurements at each moment of time t, T is the cycle duration, and $\bar{M}$ is the corresponding average value. Integrals were numerically calculated. To reduce errors due to sampling noise at least 100 average (per cycle) values were acquired and then the mean values were calculated.

1.10 Perturbation/Observation algorithm

The perturbation observation (P/O) algorithm for maximum power point tracking (MPPT) was used to optimize MFC performance during the tests with a fixed external resistor (control tests) and between frequency and duty cycle tests. At each iteration, the P/O algorithm modified R_{ext} (digital potentiometer) with a predetermined amplitude (ΔR) at each iteration. The direction of resistance change was selected by comparing the value of the power output with that at the previous resistance. Once the algorithm converges to a vicinity of the optimum resistance value, the R_{ext} will oscillate around this optimum with a maximum distance of ΔR. A computer-controlled digital potentiometer with a resistance variation range from 4 to 130 Ω and a step of 1.25 Ω was used (Innoray Inc, Montreal, QC, Canada). A detailed description of the P/O algorithm can be found in (Woodward, Perrier, & Srinivasan, 2010).

1.11 Numerical methods

Computer simulations were carried out using the equivalent circuit model and model solutions described in this document. Parameter estimation was carried out using Fmincon function of *Matlab R2010a* (Mathworks, Natick, MA, USA). In the parameter estimation procedure the root mean square error (RMSE) between the model outputs and measured values of U_{MFC} was minimized using data of five on/off cycles. At an R-PWM frequency of 0.1 Hz this corresponded to 637 data points. At a frequency of 100 Hz, 1000 data points were used to estimate model parameters.

CHAPTER 4 MFC OPERATION WITH PULSE-WIDTH MODULATED CONNECTION OF R_{EXT}

1.12 Frequency Characterisation of MFCs

In order to evaluate the effect of a pulse-width modulated connection of the external resistance (R-PWM mode of operation), MFC-1 and MFC-2 were operated at several frequencies ranging from 0.1 Hz to 1000 Hz. At each tested frequency, R_{ext} was connected to the MFC during the first half of the cycle and disconnected for the rest of the cycle, thus corresponding to a duty cycle of 50%.

Figure 2A shows the average output voltage ($\overline{U}_{ext}$) calculated over the external resistor (R_{ext}) of MFC-1 during the R-PWM tests. The frequency tests were carried out with R_{ext} values of 8 and 47 Ω. It can be seen that in all tests the average voltage increased with the initial frequency increase, then a plateau was reached at around 100-500 Hz.

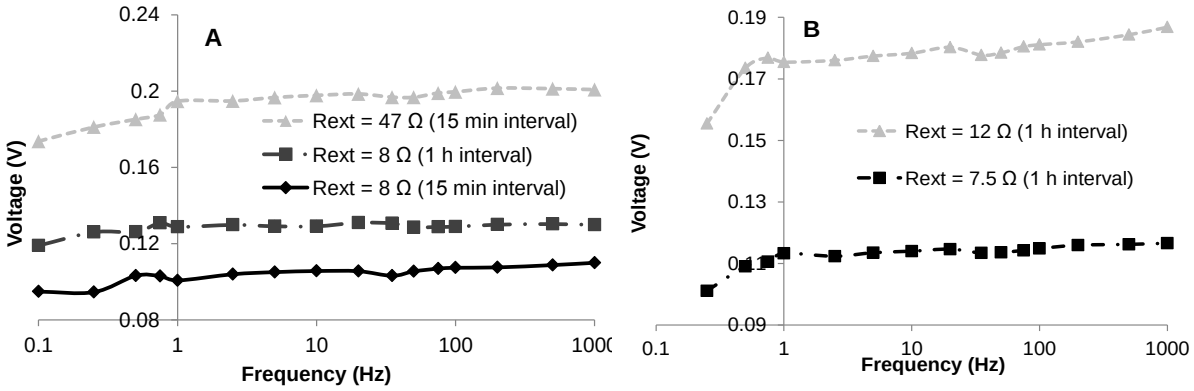

Figure 2. Average external voltage ($\overline{U}_{ext}$) as a function of Rext connection / disconnection frequency. A – MFC-1 tests with 15 min and 1 h intervals between frequency changes; B – MFC-2 tests performed with frequency changes at 1 h intervals.

Initially, frequency tests were carried out with 15 min intervals between each frequency change. The tests were also repeated with 1 h intervals between the changes. Figure 2A shows a comparison of $\overline{U}_{ext}$ profiles obtained with 15 min and 1 h intervals. It may be appreciated that profiles area qualitatively similar dependence. However, the average voltage was always higher in the tests carried out with 1 h intervals, i.e. the average (per cycle) power output was improved.

This suggests that a 15 min interval was insufficient to establish steady-state conditions corresponding to a new operating frequency. Also, it appeared that the R-PWM mode of operation led to an overall performance improvement, as power outputs were consistently higher as compared to a fixed R_{ext}. To insure reproducibility, the frequency tests were repeated in MFC-2 with R_{ext} values of 7.5 and 12 Ω.

Once again, a similar trend was observed with a near linear increase of $\overline{U}_{ext}$ as the operating frequency increased from 0.1 Hz to 500 Hz (

Figure 2B). This increase in average voltage and, accordingly, in average power output was followed by $\overline{U}_{ext}$stabilization at around 100-500 Hz.

1.13 Dynamic Response of MFCs at Low and High Frequency

MFC response to periodic connection/disconnection of R_{ext} was also characterized by observing the dynamics of MFC output voltage (U_{MFC}) during each cycle. Figure 3 compares U_{MFC} values acquired during MFC-1 operation at a low frequency of 0.05 Hz (Figure 3A, D=75%) and at a high frequency of 100 Hz (Figure 3B, D=90%).

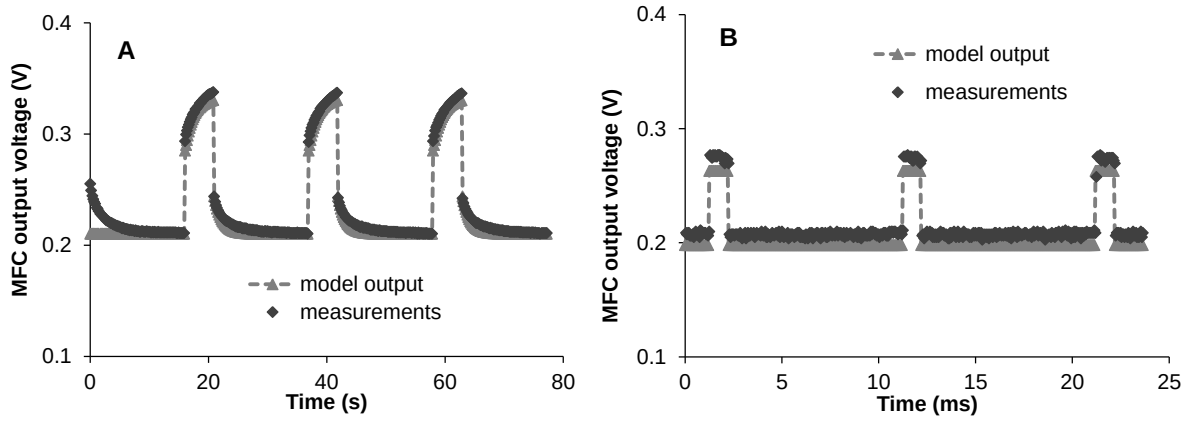

Figure 3. Profiles of MFC voltage (U_{MFC}) measured at R_{ext} connection / disconnection frequencies of (A) 0.05 Hz (D=75%) and (B) 100 Hz (D=90%).

It should be understood that when R_{ext} is connected, the output and external voltages are equal, i.e. U_{MFC} = U_{ext}. However, if R_{ext} is disconnected, then U_{ext}= 0, while U_{MFC} > 0. At both frequencies, MFC output voltage (U_{MFC}) abruptly decreases when R_{ext} is connected (closed circuit with switch ON), while it increases when R_{ext} is disconnected (open circuit with switch

OFF). Also, when R_{ext} is connected to the MFC, current demand increases and a voltage divider is created between the MFC's internal impedance and the external resistance, causing U_{MFC} to decrease.

At 0.05 Hz two different dynamics components are evidenced during each on-off or off-on transition (Figure 3A). At first, there is an abrupt change of U_{MFC} until reaching some intermediate value. This fast transition is followed by an exponential curve, which approaches the steady-state value at a much slower rate. At a frequency of 100 Hz (Figure 3B), only fast dynamics appear in the U_{MFC} curve, while the slow dynamics disappears and U_{MFC} essentially switches between two levels, with higher voltage corresponding to the open circuit state and lower voltage corresponding to the closed circuit state. This dynamics is consistent with the results of the frequency tests shown in Figure 2 and can be described by a simple equivalent circuit model (Randles model, (Randles, 1947)) previously used for modeling batteries (Durr, Cruden, Gair, & McDonald, 2006). The same equivalent circuit model was also recently used to simulate a MFC power management system (Yang, Zhang, Shimotori, Wang, & Huang, 2012). The model consists of two resistors and a capacitor, which enables the description of the slow and fast output voltage responses observed during the tests. **¡Error! No se encuentra el origen de la referencia.** shows the model diagram, where U_{OC} corresponds to MFC's open circuit voltage (ideal voltage), C represents the actual MFC capacitance, R_1 accounts for the MFC's ohmic losses, and R_2 represents the resistive component accounting for both the activation and concentration losses (Yang, Zhang, Shimotori, Wang, & Huang, 2012).

1.14 The Equivalent Circuit Model Explained

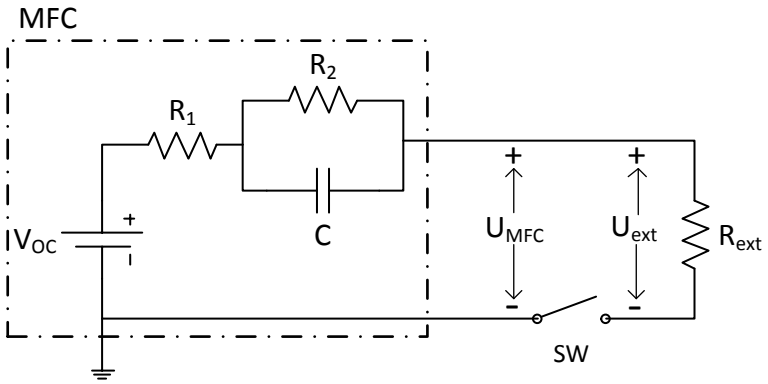

Figure 4. MFC Equivalent Circuit Model (ECM)

The following first order differential equation describes voltage dynamics over the capacitance:

$$\frac{dU_c(t)}{dt} = \frac{U_{oc}}{C(R_1 + R_{ext})} - \frac{R_1 + R_2 + R_{ext}}{R_2 C(R_1 + R_{ext})} U_c(t) \quad (2)$$

where $U_C(t)$ is the voltage at the internal capacitor, R_{ext} is the external resistance, and U_{OC} is the apparent open circuit voltage. By applying Kirchhoff's circuit law to the diagram in **¡Error! No se encuentra el origen de la referencia.**, the following analytical solution can be used to obtain MFC output voltage (U_{MFC}) as a function of time at low operating frequencies:

$$U_{MFC}(t) = \big(U_{oc} - U_c(t)\big)\frac{R_{ext}}{(R_1 + R_{ext})} \quad (3)$$

where,

$$U_c(t) = U_{final} + \big(U_c|_{t_0} - U_{final}\big)e^{-t/\tau} \quad (4)$$

Here, the capacitance final voltage U_{final} and the time constant τ are defined as:

$$\mathrm{U_{final}} = \mathrm{U_{oc}}\frac{\mathrm{R_2}}{\mathrm{R_1 + R_2 + R_{ext}}},\ \ \tau = \frac{\mathrm{R_2}}{\left(1 + \frac{\mathrm{R_2}}{(\mathrm{R_1 + R_{ext}})}\right)}\mathrm{C} \quad (5)$$

1.14.1 The High Frequency Profile

At sufficiently high frequencies of R_{ext} connection/disconnection, the voltage over the capacitance is considered to be constant, as capacitance *C* opposes to be charged or discharged. Current over the capacitance is supposed to be zero over a cycle of operation. Hence,

$$\int_0^T i_c \, dt = 0 \tag{6}$$

When the switch is closed (from *t = 0* to *t = t*),

$$i_c = \frac{U_{oc} - U_c}{R_1 + R_{ext}} - \frac{U_c}{R_2} \tag{7}$$

On the other hand, when the switch is open (from t = *t* to t = *T*),

$$i_c = -\frac{U_c}{R_2} \tag{8}$$

In this case, voltage sign changes as capacitance is supposed to discharge through resistance R_2 when the switch is open. When solving the latter integral, $U_C(t)$ may be obtained as a function of the duty cycle *D* ($^t/_T$).

$$U_c(t) = \frac{DR_2}{R_1 + R_{ext} + DR_2} U_{oc} \tag{9}$$

Then $U_{MFC}(t)$ can then be calculated as:

$$U_{MFC}(t) = U_{oc} - U_c - IR_1 \tag{10}$$

$U_{MFC}(t)$ will then vary between two values: $U_{high} = U_{oc} - U_c$ when the switch is open, and $U_{low} = U_{oc} - U_c - IR_1$ when the switch is closed. The term I represents the closed circuit current, which is given by:

$$I = \frac{U_{oc} - U_c}{R_1 + R_{ext}} \tag{11}$$

Figure 5 illustrates an example of a experimentally obtained high frequency profile of a MFC operated under R-PWM mode.

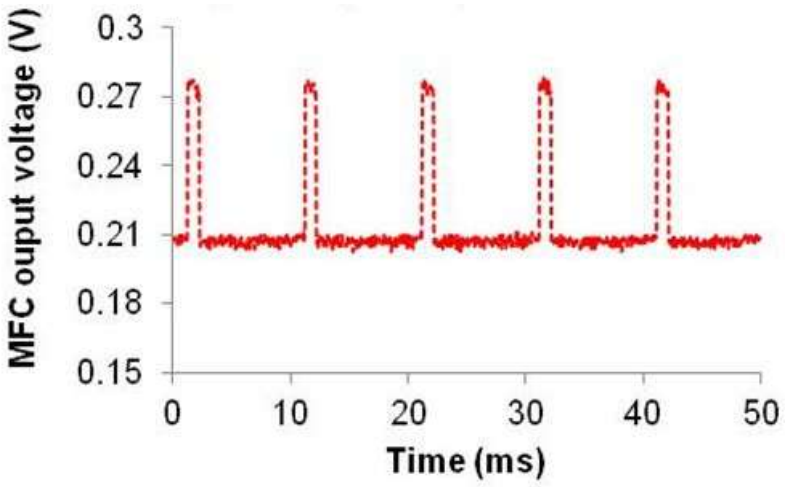

Figure 5. High frequency profile of a MFC operated under *R-PWM* mode

1.14.2 Power Analysis for High Frequency Operation

The optimal duty cycle can be found by substituting the capacitance voltage $(U_c(t))$ in equation (10) with the expression given in equation (9). Then, current is then defined as a function of duty cycle (D), as shown in equation (16) below:

$$I = \frac{U_{oc}}{R_1 + R_{ext} + DR_2} \tag{12}$$

For intermittent operation, power is defined by:

$$P = D\, I^2\, R_{ext} \tag{13}$$

The optimal value of *D* at which power output reaches its maximal value can be found from the first-order optimality condition $\frac{dP}{dD} = 0$ is evaluated. It can be seen that power output is maximized at the following value of *D*.

$$D = \frac{R_1 + R_{ext}}{R_2} \tag{14}$$

Since $R_{ext} = R_1 + R_2$ under optimal operating conditions,

$$D^* = \frac{2R_1 + R_2}{R_2} = 1 + 2\frac{R_1}{R_2} \tag{15}$$

which implies that maximal power output is achieved at D=1 (100%), at least according to equivalent circuit model analysis.

1.14.3 The Low Frequency Profile

For intermittent operation in *R-PWM* mode, R_{ext} may be equated to its true value when the switch is closed. On the other hand, when the switch is open and no current flows through the circuit, R_{ext} may be considered infinity (∞), so U_{final} may be equated to zero. Besides, the *RC* circuit time-constant becomes $\tau = R_2 C$. Finally, $U_c|_{t_0}$ is given by the value at which the capacitance is charged when the switch position is commuted. Figure 6 illustrates an example of a experimentally obtained high frequency profile of a MFC operated under R-PWM mode.

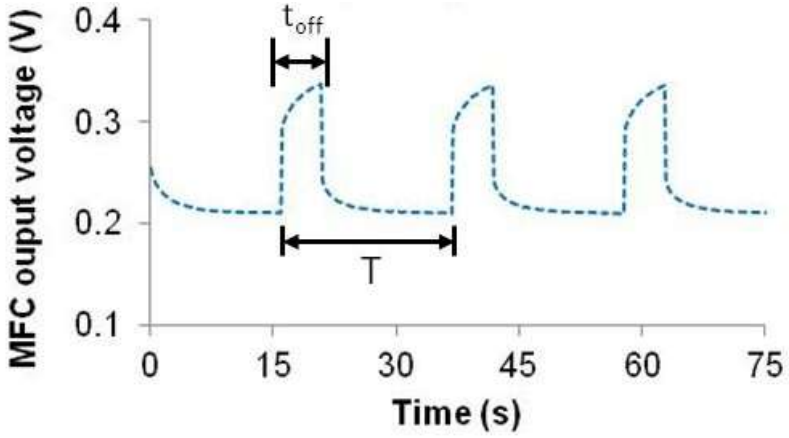

Figure 6. Voltage profile for a MFC operated at low frequency

1.15 The Proposed Equivalent Circuit as a Modeling Tool for MFCs

The proposed ECM might have a limited predictive capacity as it assumes that all the electrical elements are constant. Furthermore, this model does not consider any changes in biomass concentration, microbial activity, and carbon source concentration, i.e. constant values of these parameters are assumed. The MFC internal resistance and open circuit voltage were already demonstrated to be strongly dependent on bio-film density, on carbon source concentration in the anodic liquid, and on temperature (Pinto R. P., Srinivasan, Manuel,, & Tartakovsky, 2010.) (Pinto, Srinivasan, & Tartakovsky, 2011b.). Therefore, the equivalent circuit model might be lacking the predictive capacity of bio-electrochemical models such as recently developed two-population bio-electrochemical MFC model (Pinto R. P., Srinivasan, Manuel,, & Tartakovsky, 2010.) and the conduction-based MFC model (Marcus et al. 2007) and cannot be used to predict the influence of various process inputs, such as the organic loading rate and the operating temperature, on MFC performance.

Nevertheless, it offers some insight on the fast process dynamics linked to the electrical properties of a MFC. Indeed, when the electrical circuit is operated in the continuous mode (i.e. R_{ext} is constant), the internal capacitor is fully charged and the total internal resistance can be expressed as $R_{int} = R_1 + R_2$. The capacitor dynamics may only be evidenced when the system is disturbed, for example by means of a switch operated at a low frequency.

Figure 3 compares the equivalent circuit model outputs with voltage measurements at low (Figure 3A) and high (Figure 3B) frequencies of R_{ext} connection/disconnection. For this simulation, model parameters were estimated by minimizing RMSE between the measured voltage values and corresponding model outputs, as described above. The following parameters were estimated : U_{OC} = 0.33 V, R_1 = 4.24 Ω, R_2 = 3.25 Ω, C = 0.38 F. The comparison of simulated and measured voltage values shows that the model adequately describes process dynamics at both frequencies, although at the high operating frequency the model appears to somewhat underestimate the output voltage. As mentioned above, although process dynamics is adequately described within each cycle, the model is too simplified to predict the output voltage over extended periods of time.

Furthermore, while the equivalent circuit model analysis might suggest that the power output is maximized at *D* equal to 100%, previous studies demonstrated improved MFC power output at *D* values below 100%, at least when the MFC was operated at very low frequencies below 0.1 Hz (Grondin, Perrier, & Tartakovsky, 2012). Consequently, the performance of MFC-1 and MFC-2 was evaluated in a series of tests (*D* - tests) performed at a frequency of 500 Hz and various D values ranging from 5% to 100%, the latter corresponding to a fixed resistor.

1.16 Duty Cycle (*D*) Characterisation of the MFCs

Notably, MFC power output might also be dependent on the selected value of R_{ext}. Indeed, power output is maximized if external and internal impedances are matched. Therefore, prior to *D* tests total internal resistances (R_{int}) of MFC-1 and MFC-2 were estimated by conducting polarization tests and calculating R_{int} values using linear parts of each polarization curve. Based on this technique, both MFCs showed internal resistance values in a range of 12 - 15 Ohm.

Figure 7A shows MFC-1 power output at different values of the duty cycle and different external resistances. When *D* tests were conducted with R_{ext} = 17 Ω, which is slightly above the

estimated value of R_{int} based on the corresponding polarization test, power output was maximized at *D* = 95%. A duplicate test performed immediately after the first test demonstrated excellent reproducibility. Following this test, to compare R-PWM and mode of operation with the power output corresponding to a constant R_{ext}, MFC-1 was operated at *D* = 100% for three days. A slow decline in power output over time was observed with the power output stabilizing at 2.23 mW (Figure 7A, *D* = 100%). Interestingly, a re-evaluation of R_{int} suggested an increase to 20 Ω. A third *D* test conducted following MFC-1 operation with a constant R_{ext} confirmed a power output decrease (Figure 7A).

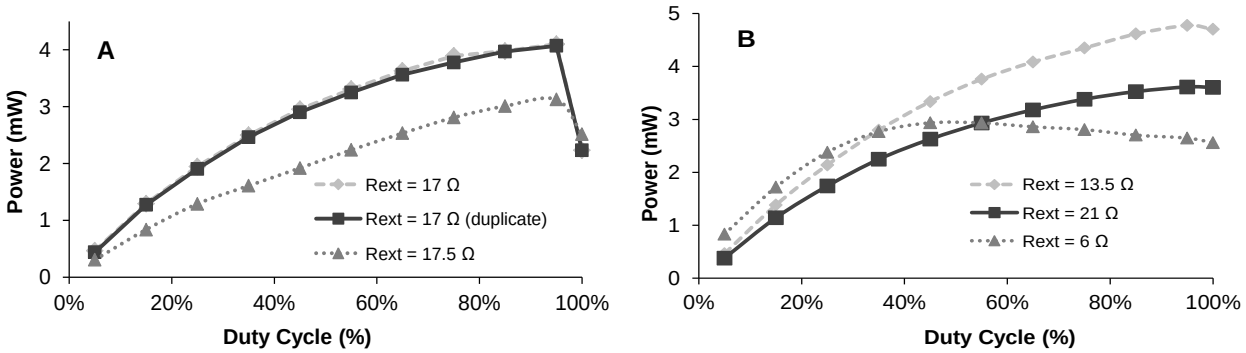

Figure 7. MFC Power outputs of MFC-1 (A) and MFC-2 (B) as a function of their duty cycles. Power output at D=100% corresponds to MFC operation with fixed external resistance. All D-tests were carried out at a frequency of 500 Hz.

D tests were also performed in MFC-2 with R_{ext} = 13.5 Ω, which corresponded to an estimated value of R_{int}. In this test, MFC power output at *D* = 100% was estimated using the same experimental procedure previously performed for other *D* values, i.e. the voltage was measured after one hour of MFC-2 operation with a fixed resistor. Consequently, the power output decrease at *D* = 100% was much lower as compared to *D* = 95% (Figure 7B). When the test was repeated at R_{ext} = 21 Ω, which was above the estimated value of R_{int}, there was no difference between power outputs at *D* = 95% and *D* = 100%. For the tests conducted at R_{ext} = 6 Ω (well below R_{int} estimation), the power output was maximized at around D = 45%, as can be seen from the data presented in Figure 7B. Although this maximum was below the highest power output observed at $R_{ext} \sim R_{int}$, the R-PWM mode of operation prevented a sharp drop in power output typically observed at $R_{ext} \ll R_{int}$. and improved MFC stability by limiting the current.

This feature might be especially useful to prevent voltage reversal in a stack of MFCs (Oh & Logan, 2007).

D-curves shown in Figure 7 are in agreement with the results presented by Grondin et al. (Grondin, Perrier, & Tartakovsky, 2012), where the external load connection was governed by the upper and lower boundaries of the MFC output voltage, thus resulting in a variable switching frequency, which was below 0.1 Hz. Overall, *D*-tests suggested an increase in power output as a result of MFC operation in R-PWM mode. To elaborate on this observation, MFC-1 and MFC-2 were operated for 3-5 days in the R-PWM mode with 95% duty cycle (100 Hz) and external resistance values chosen based on R_{int} estimations obtained in the polarization tests. Then the operating mode was changed to constant connection and the MFCs were operated for another 3-5 days. To ensure optimal performance during this period, R_{ext} value was optimized in real time using the P/O algorithm described in the Materials and Methods. This sequence of testing was repeated several times. Power outputs obtained during each MFC operation by the P/O algorithm were used as a basis for comparison (control) with the R-PWM mode of operation. The results of this comparison are summarized in Table 1 (current and power outputs were estimated based on the last 24 h of operation).

Table 1 A comparison of average currents, power outputs and Coulombic Efficiencies (CE) obtained during R_{ext} - PWM and Perturbation/Observation tests carried out at two influent acetate concentrations.

Influent acetate mg L^{-1}	**Cell**	**R-PWM mode**			**Perturbation/Observation**		
		current mA	Power mW	CE %	current mA	Power mW	CE %
900	MFC-1	16.4	3.63	91.5	14.4	2.83	80.3
900	MFC-2	13.6	3.62	76.1	14.1	2.55	78.6
1800	MFC-1	15.1	3.84	42.2	17.1	3.07	47.9
1800	MFC-2	20.6	3.60	57.6	19.6	3.46	54.9

Interestingly, similar currents (and therefore similar Coulombic efficiencies) were observed, while both in MFC-1 and MFC-2 voltages and power outputs were consistently higher during R-PWM tests. Since at an influent acetate concentration of 900 mg L^{-1} the anodic liquid measurements showed acetate – limiting conditions with acetate levels below 40 mg L^{-1}, the tests

were repeated where the influent concentration of acetate was doubled (1800 mg L^{-1}). The increased acetate load led to higher acetate concentrations in the anodic liquid (600-700 mg L^{-1}) and somewhat lower Coulombic efficiency. Nevertheless, the results given in Table 1 once again confirmed improved power output during R-PWM operation.

Overall, power outputs observed during R-PWM tests were in a range of 3.6 – 3.8 mW corresponding to a volumetric power density of 72-76 mW L^{-1}. This power density is not only higher than that observed during MFC operation using the P/O algorithm (2.6 – 3.5 mW or 51-70 mW L^{-1}, Table 1), but also is higher in comparison to the recently reported performance of a continuously operated MFC with a power density of 30-50 mW L^{-1} (Ahn & Logan, 2012).

Interestingly, the periodic and pulse modes of operation of catalytic reactors were observed to lead to an increased catalyst activity and therefore an increased volumetric performance (Silveston, Hudgins, & Renken, 1995). Several mechanisms were proposed to explain the increased catalyst activity, including a change in the catalyst state in response to reactant concentration, a higher catalyst activity due to a transient state, and non-linear reaction kinetics (Roopsingh & Chidambaram, 1999); (Silveston, Hudgins, & Renken, 1995)). While a direct comparison between the periodic operation of chemical reactors and the R-PWM mode of MFC operation might not be always justified, both systems feature catalysts with non-linear reaction kinetics. Hence, it can be suggested that at high-frequencies the R-PWM mode of MFC operation leads to a reduced activation and/or concentration losses due to changes in the bio-catalytic activity.

These losses are represented as R_2 in the equivalent circuit model (**¡Error! No se encuentra el origen de la referencia.**). Also, it can be suggested that the carbon source concentration increases when R_{ext} is disconnected. Considering poor mixing within the carbon felt anode, carbon source (acetate) transport through the porous anode might be one of the important limiting factors, i.e. acetate concentration within the anode is expected to be significantly lower than its concentration in the bulk anodic liquid.

R_{ext} disconnection prevents acetate consumption by anodophilic microorganisms. Consequently, if R_{ext} is disconnected, acetate concentration within the anode might increase to approach its level in the bulk liquid. Several previous studies demonstrated a strong link between carbon source availability and MFC performance, including the effect of carbon source on

R_{int} values (Martin, Savadogo, Guiot, & Tartakovsky, 2010) (Pinto R. , Srinivasan, Guiot, & Tartakovsky, 2011a)). As metabolic activity of the anodophilic microorganisms resumes upon R_{ext} reconnection, the improved acetate availability positively affects MFC performance. Indeed, the anodophilic microorganisms were shown to exhibit a non-linear (Monod or Haldane-like) kinetics of carbon source consumption with lower internal resistances observed at carbon source – non-limiting conditions (Hamelers, Ter, Stein, Rozendal, & Buisman, 2011); (Marcus, Torres, & Rittmann, 2007); (Manohar A. K., 2009); (Pinto R. P., Srinivasan, Manuel,, & Tartakovsky, 2010.)). These hypotheses might require extensive validation using experimental methods such as electrode potential monitoring and EIS measurements (Martin E., 2013) followed by a thorough model-based analysis.

CHAPTER 5 ECM APPLICATION FOR ONLINE MONITORING AND PARAMETER ESTIMATION OF A MFC

Commonly, electrical properties of bio-electrochemical systems are measured by means of off-line electrochemical methods like polarization curves or cyclic voltammetry. Although these methods provide highly accurate measurements for electrical parameters like internal resistance and capacitance, they require the system to be taken off-line for the measurement to be accurate.

Looking forward to applying well-known process control strategies to the enhancement of MFCs' performance, it is necessary to count on monitoring strategies that allow the online estimation/calculation of the MFCs internal parameters. Hence, the study of an online monitoring and parameter estimation strategy is presented hereafter.

This online monitoring procedure is based on both the proposed equivalent circuit model (ECM), and the low and high frequency profiles described previously. To start, the online monitoring strategy is developed. Afterwards, the laboratory tests are described. Finally, the results are presented and compared to previously developed off-line parameter estimation strategies.

1.17 Monitoring Procedure: from Electrical Modeling to Online Monitoring Tool

The analytical solution described before for the ECM can be used for online estimation of key process parameters, such as R_1, R_2, C, and U_{oc}. In the proposed procedure, R_1 is first estimated during MFC operation at high frequency (e.g. equal or above 100 Hz). Under these conditions U_c is assumed to be constant. Afterwards, U_{oc} is estimated by letting the MFC run in pseudo-open-circuit mode (R_{ext} not connected for limited time). Finally, R_2 and C are estimated when the MFC is operated at a low frequency (e.g. below 1 Hz).

In more details, at high operating frequencies U_{MFC} is assumed to be at either high (U_{high}) or low (U_{low}) levels. With respect to voltage profile in **¡Error! No se encuentra el origen de la referencia.**, the two voltage levels are related as follows:

$$U_{low} = U_{high} \frac{R_{ext}}{R_1 + R_{ext}} \quad (16)$$

Notably, U_{low} and U_{high} are measurable values, and R_{ext} is known. Hence Eq. (16) can be used for R_1 estimation. Subsequently, U_{oc} estimation can be obtained by operating the MFC in the open circuit mode for a short period of time, e.g. 60 s. In this case, U_{oc} could be assumed to be equal to the voltage at the end of the "open circuit" part of the cycle.

Furthermore, R_2 and C estimations can be also obtained using voltage measurements at low operating frequencies (e.g. T = 60 s). If the duty cycle is set at 80% in a 60 s cycle, the switch remains close during 48 seconds, making U_{MFC} decrease to a pseudo steady state value, called U_{final} in Figure 8. To facilitate the parameter estimation procedure, it is assumed that the MFC reaches a steady state voltage after 48 seconds, i.e. at the end of the cycle part with connected R_{ext}.

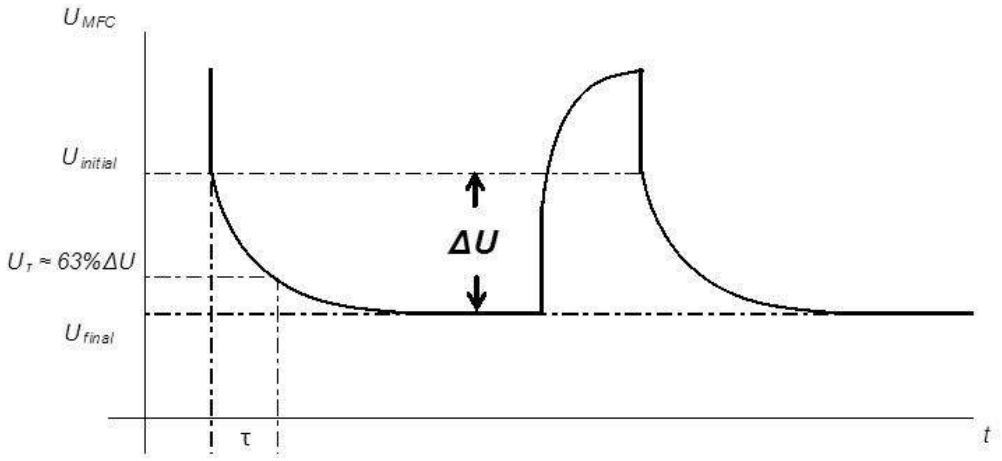

Figure 8. U_{MFC} profile at low frequency operation

The value of R_2 may then be obtained from Equation (5), as U_{final} is established experimentally, and the values for R_1 and U_{oc} have previously been estimated.

Finally, for the estimation of C, the value of τ is first established. To do so, it is calculated following the criteria that defines τ as the time that takes an exponential response to achieve the 63% of the total voltage variation. In this case, the exponential response corresponds to the impact of the capacitance dynamic behaviour over U_{MFC}, as shown in Equations (4), and (10).

In Figure 8, the exponential voltage variation is called ΔU. The fast variation of the voltage before the exponential part is not taken into account for the calculation of ΔU, as this abrupt change is attributed to the fact that the capacitance voltage does not change immediately, once the current is abruptly changed. Once τ is estimated, the value of C may be calculated from Equation (5). Five low frequency cycles are acquired, so R_2 and C are calculated as an average of the values calculated for each cycle.

1.18 Parameter Estimation and Online Monitoring Tests

To demonstrate the on-line parameter estimation procedure and compare the on-line and off-line estimations (obtained at the end of each experiment, two different tests were developed using two different MFCs.

The first test comprises the on-line monitoring and parameter estimation of a mature MFC operated at several influent concentrations of the carbon source (acetate). The second test involves monitoring of MFC start-up over time, from its inoculation to steady-state performance. For this purpose, the monitoring and parameter estimation procedure described above was implemented for a MFC which was started up and operated using the R-PWM mode.

Off-line computer simulations were carried out using the equivalent circuit model to compare the proposed on-line monitoring strategy to previously developed off-line estimated procedures. Off-line parameter estimation was carried out using Matlab R2010a (Mathworks, Natick, MA, USA). The root mean square error between the model outputs and measured values of U_{MFC} was minimized using data of five on/off cycles obtained during both low and high frequency MFC operation. All four ECM parameters were estimated when offline parameter estimation was executed using ***fmincon***.

1.18.1 MFC Internal Parameters Variation as a Function of Organic Load

MFC-1 was used for on-line parameter estimation in tests with the organic load changes imposed approximately every 3.5 days. Initially, influent concentration was set to a low value of 450 mg L^{-1}. It was then increased with step changes of 450 mg L^{-1}, until a maximum concentration of 1800 mg L^{-1} was reached. Subsequently, influent concentration was decreased with the same step change until reaching once again a minimum influent concentration of 450 mg L^{-1}. An influent concentration of 450 mg L^{-1} corresponds to an organic load of 70.65 mg d^{-1}

(hence, an acetate flow rate of 0.075 mL h^{-1}). The resulting profile of acetate flow rate is shown in Figure 9.

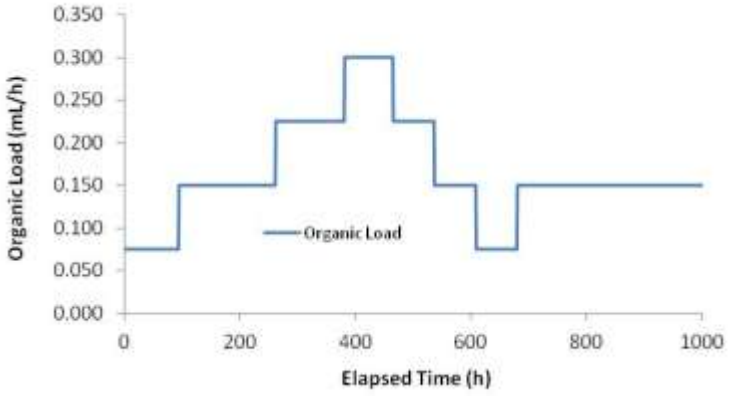

Figure 9 Flow rates of acetate stock solution

The on-line parameter estimation procedure was executed every hour, while low and high frequency profiles for U_{MFC} were acquired every 6 hours. These profiles were later used for off-line estimations.. Polarization tests were also conducted prior to each change in influent concentration. Besides, cyclic voltammetry tests were also carried out in order to estimate the MFC capacitance.

1.18.1.1 U_{MFC} profiles obtained using on-line and off-line ECM parameters

As it may be seen from the ECM analytical solutions described above, low and high frequency profiles are correlated, as values calculated at low frequency are dependant of values calculated at high frequency. Hereafter, it is shown how UMFC profiles generated from the estimated internal parameters match the actual MFC voltage profile at low and high frequencies, hence validating the proposed online monitoring approach.

Figure 10 and Figure 11 show U_{MFC} profiles obtained from offline simulations using MATLAB®. Each figure is divided into four subsections as follows:

1. Offline estimated parameters: A) U_{MFC} at low frequency, and B) U_{MFC} at high frequency,
2. Online estimated parameters: C) U_{MFC} at low frequency, and D) U_{MFC} at high frequency.

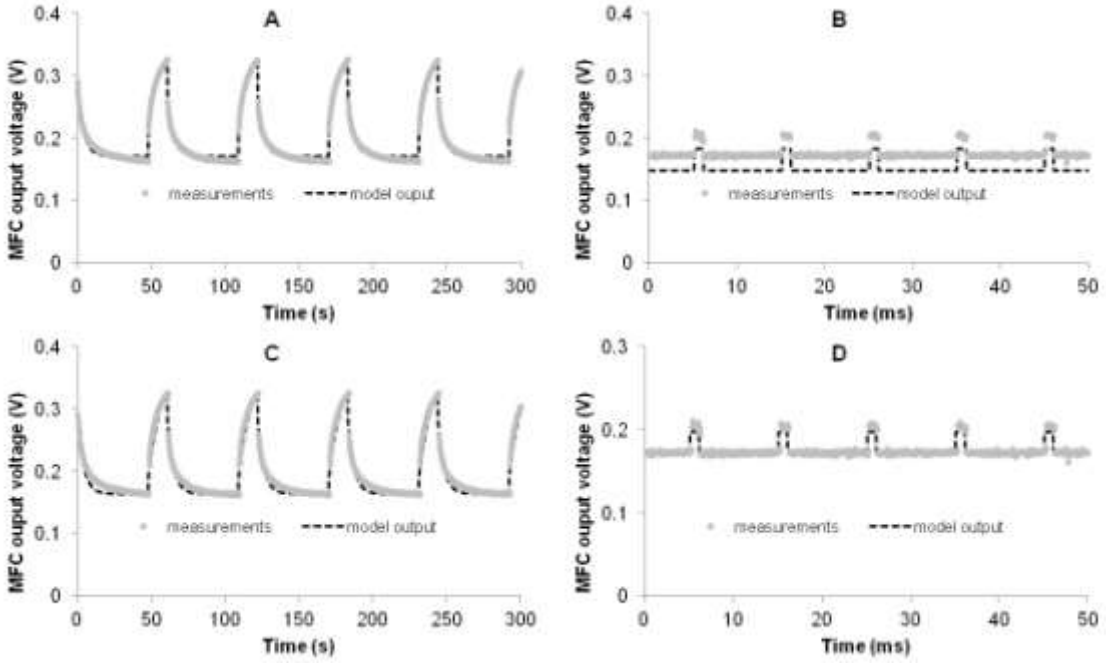

Figure 10 U_{MFC} voltage profiles at nominal or higher influent concentration (≥ 900 mg L^{-1})

As shown in Figure 10, for influent concentrations greater than the nominal value at which MFC was operated (900 mg L^{-1}), U_{MFC} profiles generated from online estimations proved to better match the U_{MFC} low and high frequency profiles than the profiles generated from offline estimated parameters. Table 2 shows a comparison of both parameter estimation procedures based on the calculation of Mean Square Errors (MSE) for each graphic in Figure 10. In the case of low frequency profiles, MSE is always smaller for offline parameter estimation. Although, online parameter estimations always proved a smaller MSE at high frequencies. As it will be discussed later, deviations were encountered in the estimations for R_2 and C.These deviations cause hence the differences in the calculated profiles.

Table 2 Mean Square Errors for UMFC estimated profiles at different organic loads

	Mean Square Error (MSE)			
	Offline Estimation		Online Estimation	
Figure	A	B	C	D
10	2.937E-05	5.260E-04	1.169E-04	9.690E-06
11	6.555E-04	3.072E-04	1.965E-03	4.500E-05

At low influent concentration, the proposed online parameter estimation strategy does not perform as well as the offline strategy. Added to inaccuracies caused by noise in the data acquisition when treating low power signals at high frequency, the procedure lacks a capacity to

replicate the low frequency profile, as capacitance values seem to be overestimated, which causes the time constant value τ to increase.

As τ is overestimated, the model might be slower than the actual dynamics (Figure 11C). On the other hand, offline estimation prove a better capacity to replicate low frequency profiles at low influent concentration (Figure 7A), although the estimation of the high frequency profile still proves to be poor (Figure 7B).

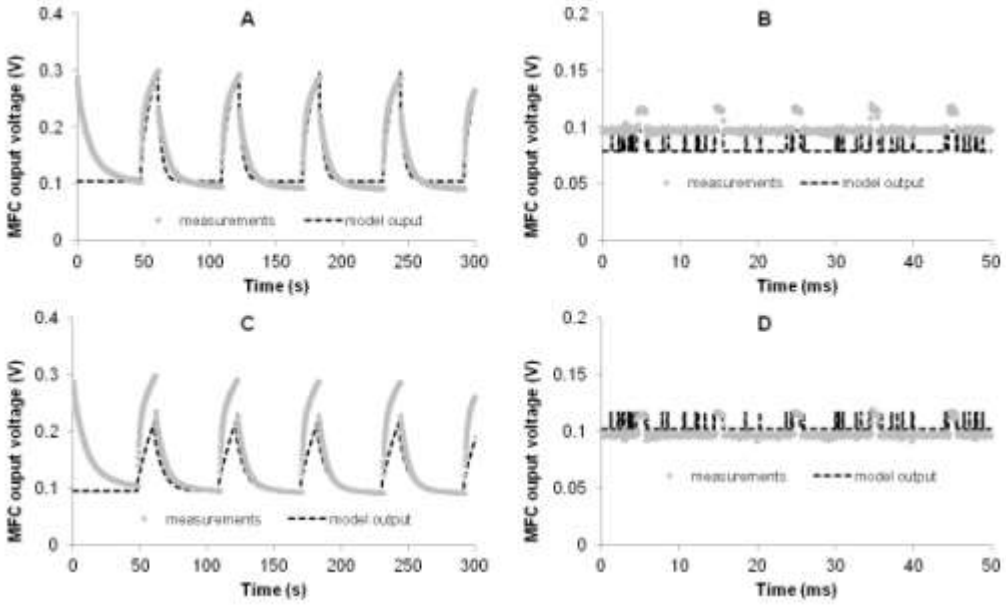

Figure 11 U_{MFC} voltage profiles at low influent concentration (450 mg L^{-1})

1.18.1.2 Comparison of On-line and Off-line Estimated Parameters

Figure 12 compares R_1 estimations obtained following the on-line estimation procedure described above with the results of the off-line parameter estimation. With an exception of a short period following MFC operation at low influent concentration (around t = 700 h), there was a good agreement between the two estimation methods. Interestingly, there was no immediate effect of influent acetate concentration (influent concentration) on the estimated R_1 value. However, MFC operation with progressively increasing influent concentrations between t = 100 h and t = 500 h led to lower R_1 values. Sharp decreases were observed around t = 180 h and then around t = 300 h (Figure 12). Shortly after the start-up of MFC operation at low influent concentration (around t = 600 h), the off-line identification procedure indicated R_1 increase, while the on-line estimation showed no significant impact (Figure 12). Both methods detected R_1

increase at around t = 850 h, which was not directly associated with a change in influent carbon source concentration.

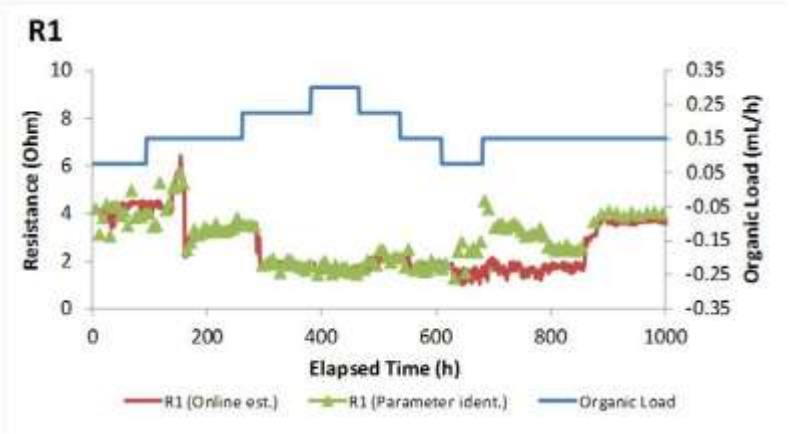

Figure 12 Results for on-line and off-line estimation of R_1

Analysis of R_2 estimations shown in Figure 13 suggested a strong link of this parameter with acetate availability in the anodic liquid. Progressive increase of the influent concentration starting from t = 100 h (Figure 13) resulted in lower values of R_2 and this trend was confirmed both by on-line and off-line estimations. Similarly, influent concentration decrease at around t = 600 h led to almost immediate increase in R_2. Interestingly, R_2 is often associated with activation losses at the anode (Yang, Zhang, Shimotori, Wang, & Huang, 2012). High activation losses might be expected at low acetate concentrations (low influent concentrations) due to carbon source - limited metabolism of anodophilic microorganisms.

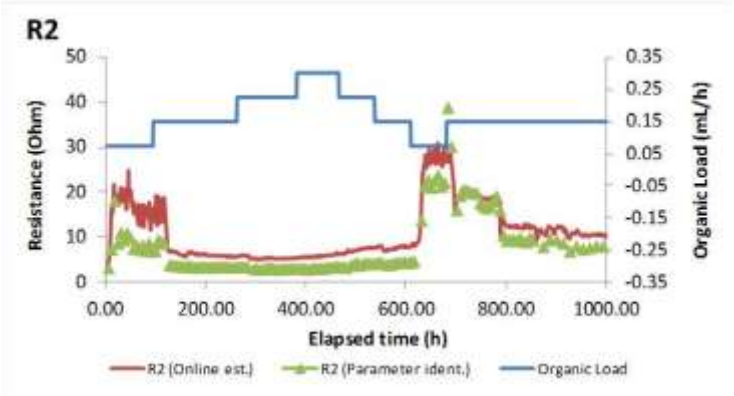

Figure 13 Results for on-line and off-line estimation of R_2

Furthermore, a comparison of model-based internal resistance estimations calculated as $R_{int} = R_1 + R_2$ with experimental results obtained in polarization tests is shown in

Figure 14. This comparison clearly confirmed the acceptable accuracy of online estimations.

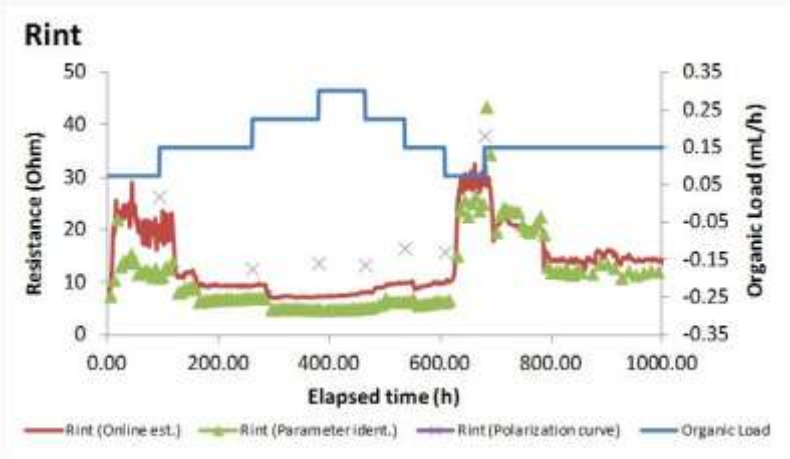

Figure 14 Comparison of Rint estimations (on-line and off-line) with experimentally measured values based on polarization tests.

In addition to R_{int} estimations, the parameter estimation procedure demonstrated carbon source – related changes in U_{oc}, as shown in Figure 15. In this case, the off-line estimation procedure appeared to provide a somewhat better response to variations in acetate load, e.g. at t = 100h (load increase) and t = 600 h (load decrease). Nevertheless, when compared with the results of polarization tests, both estimations were significantly lower than the U_{oc} values measured in the experiment with a 30 min disconnection (open circuit) period. This is to be expected, as both off-line and on-line estimation procedures were based on very short disconnection times during OFF parts of the cycles, which were clearly insufficient to achieve true steady state. Also, it should be taken into consideration, however, that long periods (dozens of minutes) of MFC operation with a disconnected external resistance might lead to carbon source accumulation in the anodic liquid, which in turn is expected to affect (increase) U_{oc} estimations.

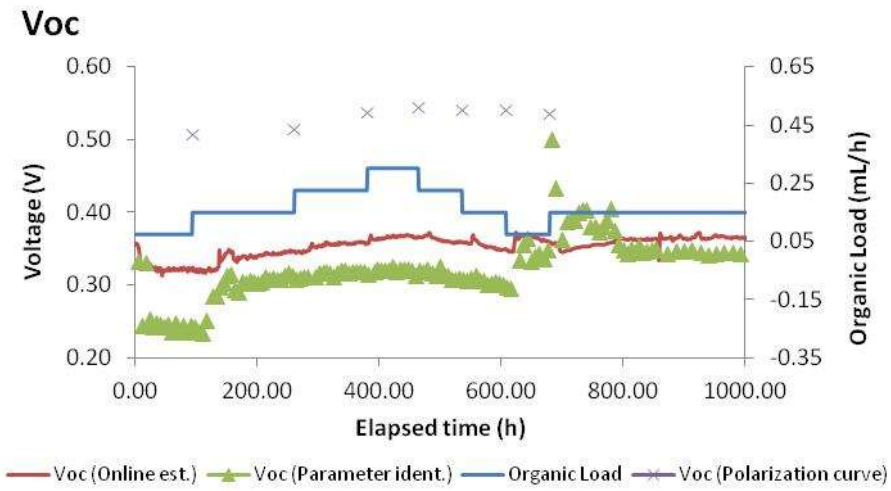

Figure 15 Results of on-line and off-line estimation of U_{oc}.

Estimated capacitance values were also studied. As can be seen in Figure 16, offline parameter identification always gave lower capacitance values than the on-line monitoring strategy proposed. Additionally, the variability of the estimated values was greater. Interestingly, online monitoring, showed that when influent concentration was decreased to a value lower than the nominal (< 900 mg L^{-1}), a fast increase in capacitance was encountered in response to such change (at times ~0 hours, and ~600 hours in Figure 16). If this response is associated to microbial capacity to storage energy, microbes seem to store as much energy as possible as carbon source is decreased and available food source is scarce. A subsequent decrease is also observed.

When influent concentration is equal or greater than the established nominal influent concentration (≥ 900 mg L^{-1}), capacitance is not greatly affected. This can be seen in the period between 150 hours and 600 hours in Figure 16. This is also confirmed by offline estimations, although the variability of the calculated parameter is greater for this period.

Finally, both online and offline estimations parameters showed a fast increase in the capacitance value when organic load was changed from low to nominal (~650 hours). Once again, as microorganisms seem to store energy after a period of famine, capacitance seems to increase as a representation of this biologic response occuring in the bioreactor. Once again, capacitance decreases after the initial increase, appearing to settle down at ~1000 hours.

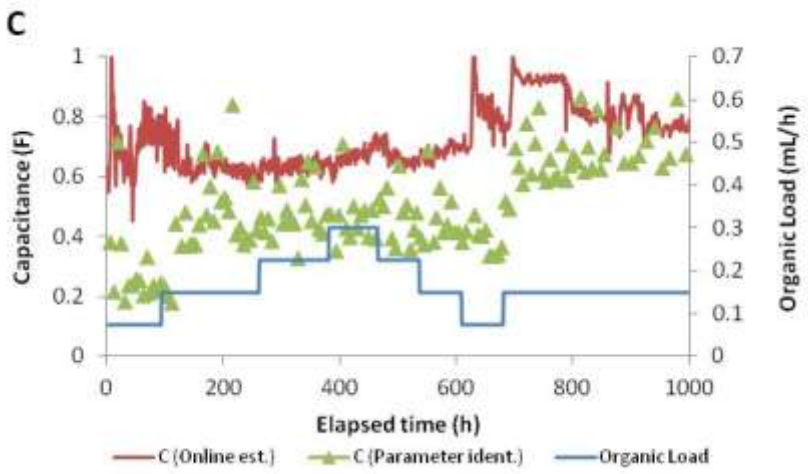

Figure 16 Results of online and offline estimation of *C*.

Table 3 shows standard deviations calculated for both online and offline estimations. As it can be seen, standard deviations are statistically similar, which proves the capacity of both the online and offline methods to represent MFC dynamics.

Table 3 Summary of Standard Deviations for Online and Offline Estimations

	Standard Deviation for Estimated Parameters	
Parameter	Online Estimations	Offline Estimations
R1 (Ω)	1.10	1.02
R2 (Ω)	6.10	6.61
Rint (Ω)	6.10	6.94
C (F)	0.10	0.16
Uoc (V)	0.01	0.04

1.18.2 MFC Internal Parameters Variation as a Function of Time

MFC-2 was used to follow variation of key MFC parameters over time. For this test, a new anode was installed and MFC-2 was inoculated with the effluent of MFC-1. MFC-2 was operated at a nominal influent concentration of 900 mg L^{-1}, and the start-up procedure involved the intermittent operation of the MFC (D = 85%, Frequency = 100 Hz), and the hourly execution of the online monitoring strategy. For this second test, U_{MFC} voltage profiles were acquired every 18 hours, and polarization tests were performed every 3 to 5 days. The test was carried out for a month, although the MFC showed signs of mature behaviour after 20 days of operation.

1.18.2.1 The Evolution of U_{MFC} Voltage Profiles in Time

Figure 17 to Figure 19 show U_{MFC} profiles obtained from offline simulations using MATLAB®. Once again, each figure is divided into four (4) as explained in 1.18.1.1. Once again, despite the inaccuracies caused by the measurement of low power signals when the MFC start-up just began, U_{MFC} profiles generated from on-line estimated parameters provided a better match to experimentally measured values.

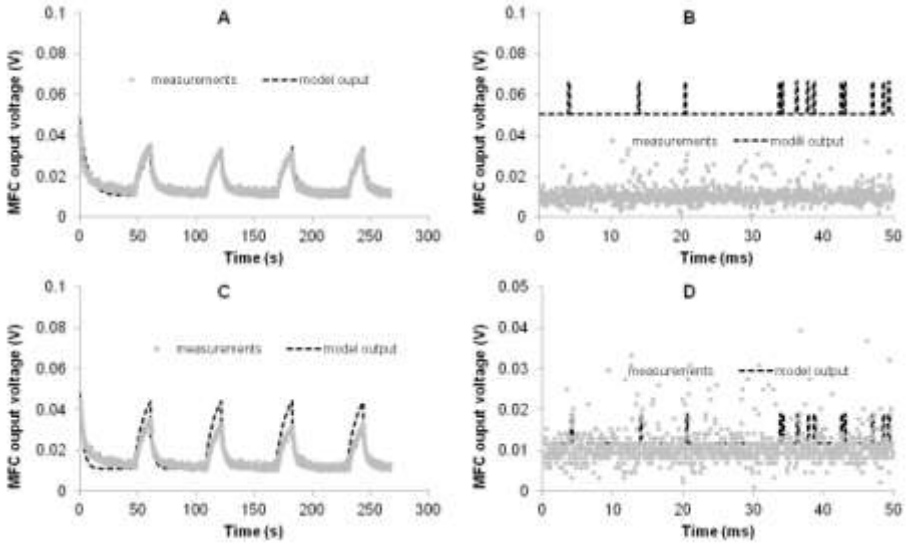

Figure 17 U_{MFC} voltage profiles 18 hours after the MFC start-up.

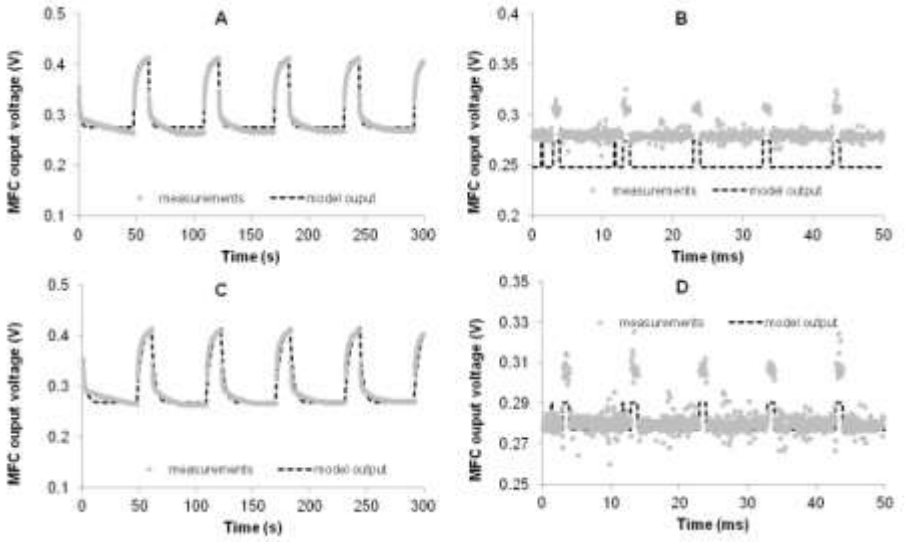

Figure 18 U_{MFC} voltage profiles 1 week after the MFC start-up.

One week after the start-up, generated profiles showed the same behaviour as when influent concentration was ≥900 mg L^{-1}. Hence, both parameter estimation strategies prove their capacity to replicate the profiles at low frequency, while the online monitoring strategy proves a to be a better tool to describe operation at high frequency. Twenty days after the MFC start-up, both parameter estimation procedures yielded similar results as shown in Figure 19. Table 4 shows MSE calculations for Figures 17, 18, and 19. Once again, offline parameter estimation shows smaller MSE values at low frequency, while MSE values at high frequency are smaller in the case of online parameter estimation.

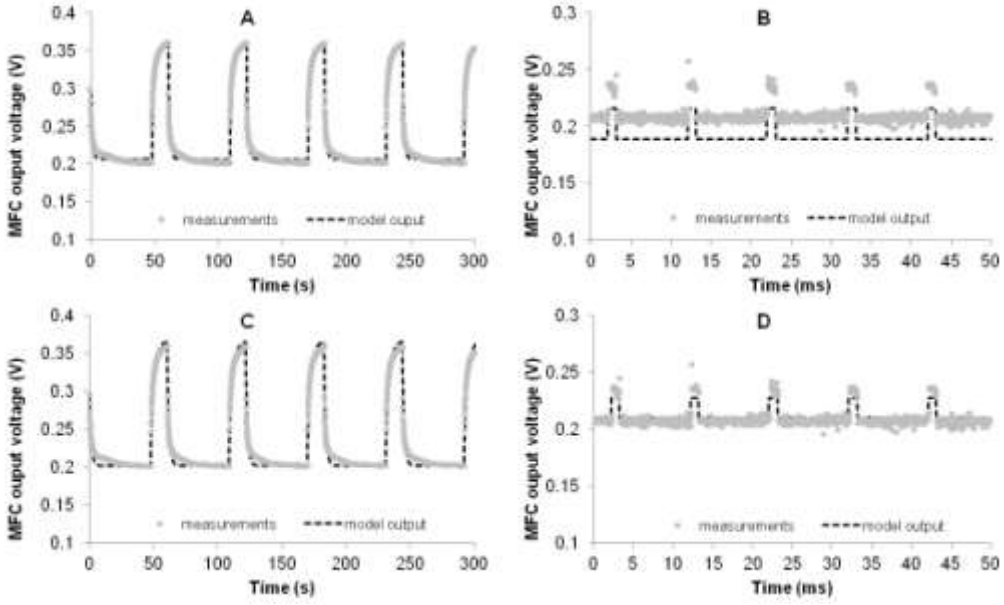

Figure 19 U_{MFC} voltage profiles 20 days after the MFC start-up.

Table 4 Mean Square Errors for U_{MFC} estimated profiles during organic maturation of MFC

	Mean Square Error (MSE)			
	Offline Estimation		Online Estimation	
Figure	A	B	C	D
17	3.715E-06	1.659E-03	1.841E-05	1.513E-05
18	5.347E-05	9.656E-04	2.026E-04	4.866E-05
19	2.122E-05	3.445E-04	7.697E-05	2.333E-05

As stated earlier in this document, one of the major challenges in bio-processes control is the development of sensors with the capacity for non-disruptive online monitoring.

The capacity of the proposed monitoring strategy to replicate the MFC electrical dynamics based on a simplified ECM opens the door to its application as a periodic follow-up sensor. Hereafter, a study of the evolution of the MFC internal parameters in time is presented.

1.18.2.2 Evolution of MFC Internal Parameters Over Time

During MFC-2 start up, internal electrical parameters were estimated every hour. Based on the values obtained, the evolution of these parameters in time was studied. Once again, U_{MFC} profiles generated from these parameters validate that the ECM is capable of replicating the MFC electrical dynamics.

Figure 20 shows the evolution of R_1 and R_2 over time. In general, R_1 values obtained from offline parameter identification were greater than those calculated from the online monitoring strategy, while values for R_2 were lower. As it could be expected, R_1 and R_2 values decrease in time. Values for R_2 were always greater than for R_1, while fairly constant values were achieved after 200 hours for R_1 and after 500 hours for R_2.

Apparently, ohmic losses (R_1) reach a steady-state value faster than activation and concentration losses (R_2). As activation and concentration losses are associated with bacteria growth and carbon source consumption, thus this kind of response over time for these two MFC internal parameters might be expected. As bacteria living cycle establishes until reaching matureness, R_2 values decrease.

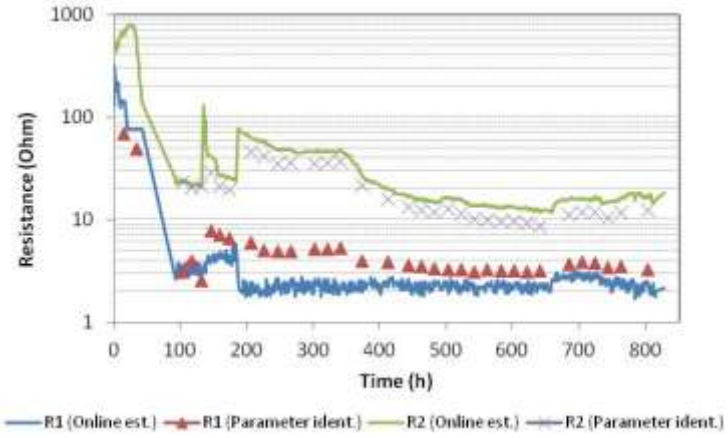

Figure 20 R_1 and R_2 evolution in time.

Internal resistance, calculated as the sum of R_1 and R_2, was compared to the values obtained by means of polarization curves. As can be seen in Figure 21, experimental R_{int} values

match well both off-line and on-line estimations. Although during 400 hours, values for Rint obtained from polarization curves and from the ECM estimations match well, after 400 hours , values calculated from the polarization curves seem to be generally greater.

As explained before, the effect of relatively long periods (dozens of minutes) of MFC operation with a disconnected external resistance may lead to carbon source accumulation in the anodic liquid, which alters bacteria behaviour, represented in the ECM by R_2, and which in turn is expected to alter the measurements for R_{int} during polarization curves tests.

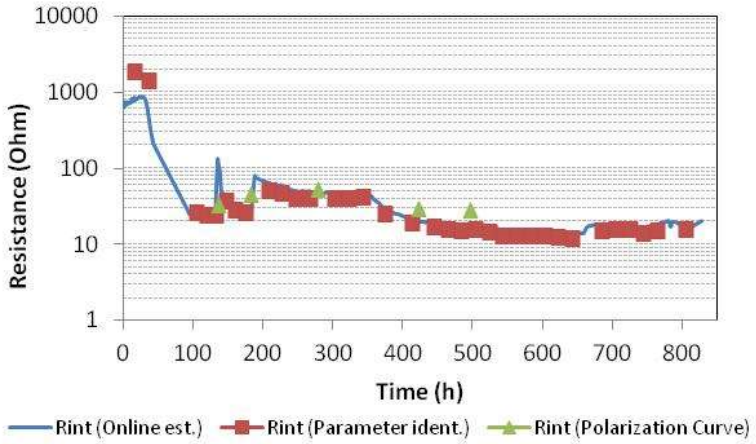

Figure 21 R_{int} evolution in time.

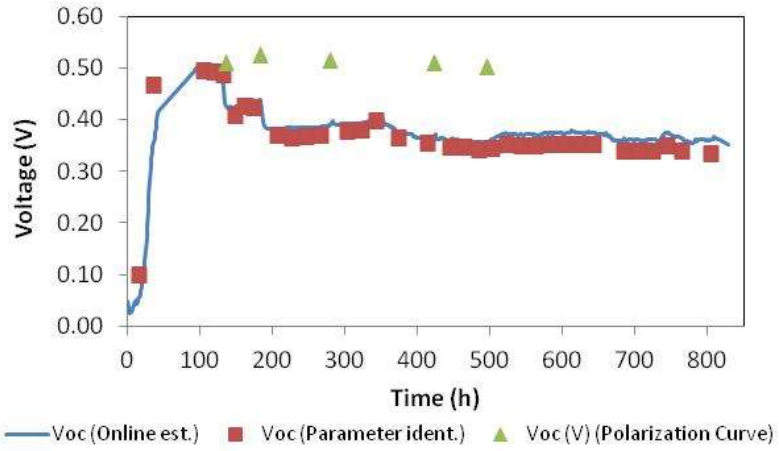

Figure 22 U_{OC} evolution in time.

In the case of U_{OC} online monitoring (**¡Error! No se encuentra el origen de la referencia.**), a fast increase was evidenced after the start up and until ~100 hours of operation. Subsequently, the value decreased almost exponentially until reaching a stable value, which was

always lower than that obtained from the polarization curves. Once again both internal parameter estimation methods gave similar results.

Finally, the evolution in time of parameter *C* was also studied, as shown in Figure 23. In this case, it was the online parameter identification routine which proved a higher variability. As it could be expected, both estimation methods showed that capacitance increases as microbial activity does. As a fact, as more bacteria grow inside the bioreactor, the greater its capacity to storage energy, what validates once again the capacitance *C* as a parameter that allows the follow-up of microbial activity for a process control purpose.

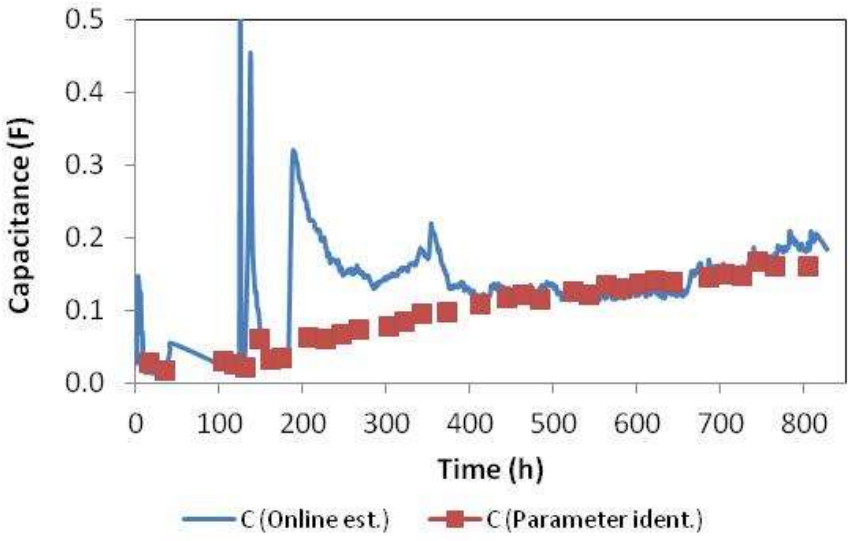

Figure 23 Capacitance *C* evolution in time.

CHAPTER 6 CONCLUSION AND RECOMMENDATIONS

1.19 Conclusions

MFC operation with pulse-width modulated connection of the external resistor (R-PWM mode) increased the average output voltage and the power output at operating frequencies above 100 Hz. By comparing power outputs of MFCs operated in the R-PWM mode and with a constant resistance equal to the estimated total internal resistance value, the R-PWM mode operation was demonstrated to improve MFC performance by up to 22-43%.

Analysis of the output voltage profiles acquired during R-PWM tests showed the presence of slow and fast dynamic components. This process dynamics was successfully simulated by a simple equivalent circuit model consisting of two resistors and a capacitor.

Furthermore, based on this simplified equivalent circuit model, an online parameter estimation strategy was implemented to periodically estimate key MFC parameters such as internal resistance, internal capacitance, and open circuit voltage. The feasibility of the proposed on-line monitoring approach was confirmed by low mean square errors (5.26E-4 for low frequency profiles, and 9.69E-6 for high frequency profiles) obtained in two laboratory trials.

Using this simple equivalent circuit model as a primary tool to develop an online estimation algorithm opens the door to further optimization of the MFCs both as a power supply or a wastewater treatment bio-system. Even if the accuracy of online estimations cannot be always verified by means of offline bio-electrochemical methods due to their interference with normal process operation, the proposed algorithm gives the capacity to follow the trends in internal parameters not only as a function of time, but also as a function of organic load variations and other external disturbances.

It is important to note that although the ECM provided adequate approximation of MFC dynamics, it lacks the capacity for long-term prediction of MFC power output (e.g. days) because it does not consider the influence of carbon source concentration and other external factors on electricity production. Furthermore, the ECM was unable to account for enhanced MFC performance at high switching frequencies. This can be seen from the comparison of MFC power outputs during operation at D=100% over a period of 2 days and at various switching frequencies, as shown in Figure 7. Higher power outputs were achieved at D values below 100%,

which is contrary to ECM analysis, which predicted optimal performance at *D*=100%. This necessitates a more detailed study on the impact of high frequency operation on MFC performance.

1.20 Recommendations

1.20.1 Characterisation of MFC performance under a wider range of frequencies

From an electrical engineering point of view, PWM is a method applied in order to regulate power to a fixed load. It is well known that power can only be maximized when *D* = 100%. However, in the case of MFC operation, power increased at *D* values below 100%.

In physiotherapy, the effect of ultrasound over living human cells has been well studied. Actually, it is well known that the application of different frequencies may have different effects on living cells. Biologists, microbiologists, and biophysicists might combine their efforts in the quest to understand bacteria performance under the effect of periodic current. The observed phenomena described in this study might be better understood and used to optimize the MFCs as a wastewater treatment tool.

1.20.2 The online monitoring strategy as a sensor for process control

Although the study of time dependant dynamics of the MFC/ECM internal parameters in response to the step changes in organic load was not in the scope of this research, these dynamics can be characterised by well-known dynamic modeling strategies, such as those using first-order models with delay.

Based on these dynamic models, PI or PID controllers can then be tuned in order to control the internal parameters while manipulating the organic load fed to the bioreactor. The control loop would consist of:

- Measurement (Sensor): In order to measure the controlled variable (any internal parameter), the online monitoring algorithm could be used as a basis.
- Decision (Controller): A digital controller whose Δt can actually be variable. This parameter is meant to be variable so estimates for the parameters can be calculated at different time intervals, and the controller would still have the capacity to compute the integral and derivative actions.

- Action (Final Control Element): An action can be taken each time a measure is executed. In this case, a dosage pump could be used, so organic load can be manipulated as a function of the flow (organic load) feeding the bioreactor.

A personal quote

Quantum physics pushed the evolution of several physics principles in a way that the human being was no longer considered to live in a world of separateness, but in a world of relationships. At the same time, science passed from being predictable (deterministic) to become pure potential (hence, statistical).

Basically, according to quantum physics, everything in this world seems to be interrelated. So, maybe, the study of living systems not only involves the application of well-known physical and engineering principles, but also of those principles that are used in daily human relationships... specially one that all living species seem to enjoy: LOVE!

Despite the initial uncertainty of working with an unknown system, I loved my work with both Margarita (MFC-1) and Juanita (MFC-2), and maybe just in response to the passion I proved (talking to them, playing music for them, sometimes even dancing to them), they gave me all the beautiful (and interesting) results included in this document. Maybe, just maybe, nature is only waiting for human species to understand that bio-systems are living species willing to serve our purpose.

Although, as the interaction of interrelated species, love will have to become a headstone in the understanding of all biology 'equations'. Of course, modeling love seems a bit of a challenge (for now!), but for sure, lots of love can be given to those magic bacteria who have already proven their capacity to treat water, while they recover electrical energy out of 'waste'.

BIBLIOGRAPHY

Aelterman, P., Rabaey, K., Pham, H. T., Boon, N., & Verstraete, W. (2006). Continuous electricity generation at high voltages and currents using stacked microbial fuel cells. *Environmental Science and Technology, 40,* 3388-3394.

Aelterman, P., Versichele, M., Marzorati, M., Boon, N., & & Verstraete, W. (2008). Loading rate and external resistance control the electricity generation of microbial fuel cells with different three-dimensional anodes. *Bioresource Technology, 99,* 8895-8902.

Ahn, Y., & Logan, B. (2012). A multi-electrode continuous flow microbial fuel cell with separator electrode assembly design. *Appl Microbiol Biotechnol 93*, 2241-2248.

Bae, W., & Rittmann, B. E. (1996a). Responses of intracellular cofactors to single and dual substrate limitations. *Biotechnology and Bioengineering, 49,* 690-699.

Bastin, G., Bernard, O., Dochain, D., Génovési, A., Gouzé, J.-L., Harmand, J., . . . Vanrolleghem, P. (2001). *Automatique des bioprocédés.* Paris: Hermès Science Publications.

Bergman, T. L., Lavine, A. S., Incropera, F. P., & Dewitt, D. P. (2012). *Introduction to Heat Transfer.* John Wiley & Sons, Inc.

Coronado, J., Perrier, M., & Tartakovsky, B. (2013). Pulse-width modulated external resistance increases the microbial fuel cell power output. *Bioresource Technology*.

Debabov, V. G. (2008). Electricity from Microorganisms. *Microbiology*, 149-157.

Degrenne, N., Buret, F., Allard, B., Bevilacqua, & P. (2012). Electrical energy generation from a large number of microbial fuel cells operating. *Journal of Power Sources 205*, 188– 193.

Dewan, A., Donovan, C., Heo, D., & Beyenal, H. (2010). Evaluating the performance of microbial fuel cells powering electronic devices. *Journal of Power Sources 195,* 90-96.

Durr, M., Cruden, A., Gair, S., & McDonald, J. R. (2006). Dynamic model of a lead acid battery for use in a domestic fuell cell system. *J. Power Sources, 161,* 1400-1411.

Eddy, M. (2003). *Wastewater Engineering: Treatment and Reuse.* New York, NY: McGraw-Hill Science/Engineering/Math.

EG&G Technical Services, Inc. (2004). *Fuel Cell Handbook.* Morgantown, West Virginia: U.S. Department of Energy.

Grondin, F., Perrier, M., & Tartakovsky, B. (2012). Microbial fuel cell operation with intermittent connection of the electrical load. *Journal of Power Sources, 208,* 18-23.

Hamelers, H. V., Ter, H. A., Stein, N., Rozendal, R. A., & Buisman, C. J. (2011). Butler-Volmer-Monod model for describing bio-anode polarization curves. *Bioresource Technol. 102*, 381-387.

Kim, J. R., Rodríguez, J., Hawkes, F., Dinsdale, R., Guwy, A., & Premier, G. (2011). Increasing power recovery and organic removal efficiency using extended longitudinal tubular microbial fuel cell (MFC) reactors. *Energy & Environmental Science*, 459-465.

Logan, B. E., Hamelers, B., Rozendal, R. A., Schroder, U., Keller, J., & Freguia, S. (2006). Microbial Fuel Cells: Methodology and Technology. *Environmental Science and Technology, 40*, 5181-5192.

Logan, B., & Regan, J. M. (2006). Electricity-producing bacterial communities in microbial fuel cells. *Trens in Microbiology*, 512-518.

Manohar A. K., M. F. (2009). The internal resistance of a microbial fuel cell and its dependence on cell design and operating conditions. *Electrochim. Acta 54*, 1664-1670.

Marcus, A. K., Torres, C. I., & Rittmann, B. E. (2007). Conduction-based modeling of the biofilm anode of a microbial fuel cell. *Biotechnol. Bioeng. 98,*, 1171-1182.

Martin E., S. O. (2013). Electrochemical characterization of anodic biofilm development in a microbial fuel cell. *Appl. Electrochem. 43*, 533-540.

Martin, E., Savadogo, O., Guiot, S. R., & Tartakovsky, B. (2010). The influence of operational conditions on the performance of a microbial fuel cell seeded with mesophilic sludge. *Biochem. Eng. J. 51*, 132-139.

Oh, S. T., Kim, J. R., Premier, G., Lee, T. H., Kim, C., & Sloan, W. (2010). Sustainable wastewater treatment: How might microbial fuel cells contribute. *Biotechnology Advances, 28*, 871 - 881.

Oh, S.-E., & Logan, B. E. (2007). Voltage reversal during microbial fuel cell stack operation. *J. Power Sources 167*, 11-17.

Park, J.-D., & Ren, Z. (2012). High efficiency energy harvesting from microbial fuel cells using a synchronous boost converter. *Journal of Power Sources, 208*, 322-327.

Park, J.-D., & Ren, Z. (2012). Hysteresis controller based maximum power point tracking energy harvesting system for microbial fuel cells. *Journal of Power Sources, 205*, 151-156.

Picioreanu, C., Katuri, K. P., Head, I. M., Van Loosdrecht, M. C., & Scott, K. (2008). Mathematical model for microbial fuel cells with anodic biofilms and anaerobic digestion. *Water Science & Technology*, 965-970.

Pinto, R. P., Srinivasan, B., & Tartakovsky, B. (2011b.). A unified model for electricity and hydrogen production in microbial electrochemical cells. *18th IFAC Word Congress.* Milano, Italy.

Pinto, R. P., Srinivasan, B., M. M.-F., & Tartakovsky, B. (2010.). A two-population bio-electrochemical model of a microbial fuel cell. *Bioresource Technol*, 5256-5265.

Pinto, R., Srinivasan, B., Guiot, S., & Tartakovsky, B. (2011a). The Effect of Real-Time External Resistance Optimization on Microbial Fuel Cell Performance. *Water Research*, 1571-1578.

Pinto, R., Tartakovsky, B., Perrier, M., & Srinivasan, B. (2010). Optimizing Treatment Performance of Microbial Fuel Cells by Reactor Staging. *Ind. Eng. Chem. Res.*, 9222-9229.

Premier, G. C., Rae Kim, J., Michie, I., Dinsdale, R. M., & Guwy, A. J. (2011). Automatic control of load increases power and efficiency in a microbial fuel cell. *Journal of Power Sources, 196,* 2013-2019.

Randles, J. E. (1947). Kinetics of rapid electrode reactions. *Disc. Faraday Soc.*, 11-19.

Roopsingh, G., & Chidambaram, M. (1999). Periodic operation of bioreactors for autocatalytic reactions with Michaelis-Menten kinetics. *Bioprocess Eng. 20*, 279-282.

Saito, T., Mehanna, M., Wang, X., Cusick, R. D., Feng, Y., & Hickner, M. A. (2011). Effect of nitrogen addition on the performance of microbial fuel cell anodes. *Bioresource Technology, 102*, 395–398.

Silveston, P., Hudgins, R. R., & Renken, A. (1995). Periodic operation of catalytic reactors - introduction and overview. *Catalysis Today, 25*, 91-112.

Woodward, L., Perrier, M., & Srinivasan, B. (2010). Comparison of Real-Time Methods for Maximizing Power Output in Microbial Fuel Cells. *AIChE Journal, 56*(10), 2742-2750.

Woodward, L., Perrier, M., Srinivasan, B., & Tartakovsky, B. (2009). Maximizing Power Production in a Stack of Microbial Fuel Cells Using Multiunit Optimization Method. *AIChE Journal, 25*(3), 676-682.

Wu, P. K., Biffinger, J. C., Fitzgerald, L. A., & Ringeisen, B. R. (2011). A low power DC/DC booster circuit designed for microbial fuel cells. *Process Biochemistry*.

Yang, F., Zhang, D., Shimotori, T., Wang, K.-C., & Huang, Y. (2012). Study of transformer-based power management system and its performance optimization for microbial fuel cells. *Journal of Power Sources, 205*, 86-92.

Zhang, X.-C., & Halme, A. (1995). Modeling of A Microbial Fuel Cell Process. *Biotechnology Letters 17,* 809-814.